FABRICATION OF MEMBRANES USING SOL-GEL CHEMISTRY ON GLASS
CHIPS AND PROTEIN SEPARATIONS USING ON-COLUMN FLUORESCENCE
LABELING BY CAPILLARY ELECTROPHORESIS

by

YUEPING CAO

M.S., Lanzhou Institute of Chemical and Physics, CAS, 2000

A THESIS

submitted in partial fulfillment of the requirements for the degree

MASTER OF SCIENCE

Department of Chemistry
College of Arts and Sciences

KANSAS STATE UNIVERSITY
Manhattan, Kansas

2007

Approved by:

Major Professor
Christopher T. Culbertson

Abstract

The field of microfluidic devices has being developed quickly. It is aimed at integration of many chemical functions in a single chip, such as sample pretreatment, preconcentration, separation and detection, which provides a number of advantages including simplicity, automation, reduced analysis time, decrease in amount of samples and reduced formation of waste. Its potential applications have been conducted in the fields such as biotechnology, pharmaceuticals, life sciences, public health, agriculture and related areas.

Membrane technology has been applied in analytical chemistry for many years and has won substantial growth in microfluidics over the past 10 years. Membrane is used to control transfer of some kinds of species, which can be employed for sample concentration, sample preparation, sample filtration and microreactors and so on. Sol-gel process, which usually involves catalytic hydrolysis of sol-gel precursor(s) and catalytic polycondensation of the hydrolyzed products and other sol-gel-active components present in the reaction medium to form a macromolecular network structure, is one of the most suitable methods for membrane fabrication. In this work, titanium membrane was fabricated inside glass microchips using the precursor of titanium isopropoxide. The resulted membranes demonstrated the excellent preconcentration effect. Followed separation and detection were also achieved.

CE has been highly accepted as an efficient separation technique for qualitative and quantitative determination, which is performed using a narrow-bore capillary tube. It offers advantages of simplicity, high resolution separation, and minimal cost in terms of analysis time and sample consumption. In this work, protein separations were carried out by CE. Laser-induced fluorescence was used as detection. On-column fluorescence labeling using a fluorogenic labeling reagent was made. Under suitable experimental conditions, an excellent separation performance with about 1.4 million theoretical plate numbers was achieved.

Table of Contents

List of Figures

List of Tables

Acknowledgements

I would like to thank my research advisor Dr. Christopher Culbertson for his guidance and wisdom. I want to express my gratitude to my supervisory committee, Dr. Paul Smith and Dr. Eric Maatta for their support. I would also like to thank all the people who have helped me during my study here, teachers, department staff and friends, especially people at Dr. Culbertson's group. Without their effort and help, this work would have been very difficult. I also want to show my acknowledgement to all the other faculty and graduate students at the department of chemistry. Their advice and help was invaluable asset for me. I thank the department of chemistry and Kansas State University for the opportunity given to me to pursue study here.

 I would love to thank my parents in China. Their unselfish love and support is the main drive for me to have faced the difficulties I have met in my life and study.

In addition, I would like to extend my appreciation to all the friends I have made in Manhattan. Thank them for their help with my study and life in here. Their friendship and understanding will be memorized in my heart forever.

Dedication

This thesis is dedicated to my parents, Guizhi Yang and Wenshan Cao. Thank them for their encouragements, support and belief in me.

CHAPTER 1 - Fabrication of Membranes on Microfluidic Devices Using Sol-gel Chemistry

1.1 Introduction
1.1.1 Microfluidic Devices
1.1.1.1 Background of Microfluics

Microfluidics refers to a set of technologies that control the flow of minute amounts of liquids or gases—typically measured in nano- and picoliters—in a miniaturized system, that is, microfluidic devices (1). The concept, also called lab-on-a-chip (LOC) or micro total analysis system (μ-TAS) which was proposed by Manz et al.(2) is focused on miniaturization and integration of many functions on a single chip, such as purification, derivatization, reaction, separation (e.g., chromatography, electrophoresis), detection and incorporating control of mass transport and measurements. Microfluidic devices can be identified by the fact that they have one or more channels with at least one dimension less than 1mm (3). They were first developed in the early 1990s (4)and initially focused on flow through simple channel layout and fabricated in silicon and glass using photolithography and etching techniques, which are precise but expensive and inflexible. The development of microfluidics has been directed towards almost hands-free chemical and biochemical analysis on microfluidic devices. Designs of microfluidic devices have become much more complex and the trend of fabrication methods has changed to soft lithography based on printing and molding organic materials, allowing the construction of three-dimensional networks of channels and components and providing a high level of control over the molecular structure of channel surfaces.

The field of microfluidic devices is reminiscent of the invention of capillary electrophoresis in 1979, which uses fused silica capillary to offer a separation compartment for researchers to drive liquid chromatography and capillary electrophoresis in μm-sized channel dimensions. Microfluidic devices go one step further by etching an entire separation manifold on a planar wafer, providing additional intersecting channels and almost unlimited possibilities for realizing relevant analysis on a single chip(5) and thus providing the advantage of integration with other microfluidic functions over traditional capillary system. Early research on

the miniaturization concept indicated that electroosmotic flow was a feasible method to drive liquid samples through interconnected channels in a microfluidic device, especially for separation (2). Experimental efforts were put to develop micropump systems (6) and sample injectors (7) to transport samples through channels and directed to optimize injection and separation. Harrison and coworkers (8) first demonstrated the viability of integration of electrophoresis in a planar chip as a chemical analysis system for sample separation and solvent pumping and proved the feasibility of utilizing electroosmotic pumping for transport control in interconnected channels without using valves. Subsequently a variety of electrophoretic separation modes were applied on microfluidic devices. Capillary electrophoresis (CE) in addition to capillary gel electrophoresis, micellar electrokinetic chromatography, electrochromatography have adapted to microfluidic devices for electrokinetic driven separation. Capillary electrophoresis has been widely applied to microchips (9) and on-chip capillary electrophoresis (CE) has been the subject of extensive study over the past decade (10). Woolley et al. designed and fabricated capillary array electrophoresis system which was able to analyze and detect 12 different DNA samples in parallel, proving to be useful for high-throughput genotyping (11). Micellar electrokinetic capillary electrophoresis of some samples was demonstrated on glass chips (12, 13).

1.1.1.2 Basic Principles of Microfluidics (14, 15)

The flow of a fluid in a microchannel can be characterized by the Reynolds number, used to characterize laminar and turbulent flow regimes and defined as

$$R_e = L V_{avg} \rho / \mu$$

Where L = Channel depth or width

μ = viscosity

ρ = fluid density

V_{avg} = average velocity of the flow

Due to the small dimensions of microchannels, R_e is usually much less than 1, often less than 0.1. In this Reynolds number regime, flow is completely laminar and no turbulence occurs. The transition to turbulent flow generally occurs in the range of Reynolds number 2000. Laminar flow provides a means by which molecules can be transported in a relatively predictable manner through microchannels. When two laminar flow fluid streams meet, they simply mix by diffusion alone, which can be

used to generate concentration gradients. The Einstein-Smoluchowski equation ($\sigma^2 = 2Dt$) describes diffusion in one dimension. Here σ, D, t stand for variance, diffusion coefficient, and time assuming a Gaussian diffusion profile. The variance can be considered as the distance a particle or molecule moves in the time element t. The squared dependence of the spatial motion of a molecule is very important at the micro- and nano- scale. For example, it needs to take about a billion seconds for Lysozyme to diffuse 1 cm, while it only takes it 1 second to diffuse 10μm. This fact has been used thoroughly in biological systems with nano- or micro- scale.

Note, however, that even at Reynolds numbers below 1, it is possible to have momentum-based phenomena.

There are two common ways used to achieve fluid pumping through microchannels. They are pressure driven flow and electrokinetic flow. For pressure driven laminar flow, the so-called no-slip boundary condition, one of the basic laws of fluid mechanics states that the fluid velocity at the channel walls must be zero. Thus a parabolic velocity profile within the channel is produced.

Electroosmotic flow pumping (EOF) is another technique for pumping fluids. Electroosmotic flow plays a key role in the concept of microfluidic system. An electric double layer of counter ions can be generated at the walls of most surfaces which have an electric charge. A potential difference will be formed within the double layer. When an electric field is applied across the channel, the ions in the double layer move towards the electrode of opposite polarity. Their movements will drag the bulk fluid to move toward the same direction, resulting in that all cations and anions move in the same direction, creating a flat flow profile in which the velocities are uniform across the whole width of the channel. One benefit of EOF is that it doesn't directly contribute to sample dispersion in the form of band broadening. The detailed EOF mechanism will be discussed in chapter 2.

1.1.1.3 Applications and the Future of Microfluidic Devices

The use of microfluidic devices offers many significant advantages. Since it holds the promise of integrating multiple chemical processing steps on single chip, it can provide the following advantages: automation, reduced consumption of samples, decrease in waste generation, high-speed analysis, operational simplicity, and etc (14).

Mirofluidic devices can be used to obtain many interesting measurements, such as chemical binding coefficients (15), molecular diffusion coefficients (15), pH (16) and enzyme reaction kinetics (17). A T-sensor, a recently developed microfluidic device, exploits low Reynolds number flow conditions and optically monitors the interdiffusion and chemical interaction of components from two or more fluid streams, allowing measurements of sample concentrations on a continuous basis and determination of diffusion coefficients and reaction rate constants (15). Gradients of pH were electrochemically formed and optically quantified in microfluidic channels using acid-based indicators, and pH can be measured.

Microfluidic devices have also found a large variety of ways in biological and clinical research. These applications include flow cytometry (18), immunoassays (19, 20), DNA analysis (21, 22), cell manipulation (23), cell separation (24), and cell patterning (25) and so on. Much of the research has the utility for clinical diagnostic. Thus commercial microfluidic analysis principles are pushing strongly into pharmaceutical and biotech research. Dispensing technologies for micro-well plate liquid handling management have been applied in pharmaceutical screening (3). Microarrays are becoming prime tools for genomic and proteomic study. Classic sensor and separation principles are also aimed for commercial applications. Ink-jet printing exploits orifices with a diameter of less than $100\mu m$ to generate drops of ink and it is the most mature application of microfluidics, which has been used to deliver reagents to microscopic reactors and deposit DNA into arrays on the surface of microfluidic devices.

No industry standard exists for microfluidic devices although they are winning the market. The area remains open for exploration and its potential offers the diving force behind new innovations and research in academic and industry (1).

Glass microchips were used in this work. Their design and fabrication method will be presented in the experimental section.

1.1.2 Sample Preconcentration
1.1.2.1 Background

Developments in microfluidics have made it possible to fabricate devices with increased functionality and complexity for chemical and biochemical applications (1).

To produce arrays of separation channels for high-throughput applications is a potential advantage of microfluidic devices, in addition to integration and multifunctionality (1). As with many analytical separation techniques; microfluidic systems also need very sensitive detection methods, especially for analysis of trace species in complex mixtures. Many detection methods such as UV absorbance detection, laser-induced fluorescence have been applied to the integrated microstucture systems. However, the small injection volume of a sample and the short path length for optical measurements degrade separation efficiency and separation resolution. Some methods including using Z-cells and U-shaped cells or widening the capillary at the detection position were developed to enlarge detection path length and they were able to improve detection limits (26, 27). Due to the detection limits of these methods, another common strategy, which is the species of interest are concentrated before separation has been widely studies and demonstrated. For electrokinetically driven flow separation mode, sample stacking and field amplification stacking has been performed. Kutter and co-workers presented sample stacking and on-chip complexity for the purpose to increase the sensitivity of detection of their microchip system combined with capillary electrophoresis (28). Lichtenberg et al. demonstrated field-amplified sample injection of long plugs of samples with about 65- fold increase in signal (29). In the paper of Gong et al. (30), preconcentration was achieved using a sample buffer injection, followed by field-amplified stacking injection with sample buffer removal from the separation channel on a glass chip. Isotachophoresis was studied on glass chip by integrating a laser system to allow detection of the zone boundaries (31). The isoelectric focusing was performed by using pressure mobilization (32).Computer-controlled differential electroosmotic pumping of aqueous and organic phases to produce solvent gradients and flows was achieved; and thus the composition of the solvent and the anlayte is changed by ramping the concentration of solvent A and B from proportion of m and n to proportion of n and m (33). Kim and coworkers constructed a protein concentration microfluidic device using a simple one-layer fabrication process with a hypothesis that a nanoscale channel whose exclusion-enrichment effect resulted in concentration formed between the two substrate layers(34).

1.1.2.2 Stacking Principles

Sample stacking is a general term for methods in CE which are exploited for on-line concentration of diluted samples (35). During stacking, a long injected sample zone in which analytes present at lower concentrations is transformed into a short zone with analytes with higher concentration due to stacking. Electromigration phenomena or chromatographic effects can be utilized to carry out the conversion of a long sample zone into a short one. The major principle of stacking in electrophoresis is manipulation of net migration velocity. It follows the mass conservation principles in electrophoresis when a substance migrates into a region where its net velocity is decreased, its concentration will be increased.

In order to create stacking, the analyte zone and the stacking zone should stay in contact at least until the stacking of all the injected analyte is finished. Several stacking modes have been applied. First, the principle of conservation of the Kohlrausch regulating function (KRF) is followed at any point of the channel. For monohydric strong and weak acids and bases, it can be expressed as

$$\Sigma \ \bar{c_i} / \ \bar{u_i} = \text{constant}$$

Where $\bar{c_i}$ = the concentration of component i

$\bar{u_i}$ = the ionic mobility of component i

This formula means the concentration of an analyte is automatically adjusted to match the local KRF value. Second, step of pH is applied to weak acids and bases. Their mobility is a function of pH. For instance, when a base migrates into a zone of low pH, it is fully protonated and migrates towards a region of higher pH, resulting in decrease in ionization degree and a lower migration velocity and stacking. Formation of complexes and can also be used to control the effective mobility by changing the charge of an analyte. Chromatographic accumulation works in a similar way. For example, micellar solutions are used to incorporate an analyte and reduce its effective mobility. For boundary stacking mode, a self-sharpening boundary is generated by using one component only at one side of the boundary. The boundary stays sharp if the velocity of the analyte behind the boundary is smaller than that of the boundary.

In this work, membrane technology is mainly employed for sample preconcentration. Therefore this method of preconcentration in microfluidics will be reviewed in the next section separately.

1.1.3 Preconcentration Using Membrane

1.1.3.1 Background

Membrane science and technology is a broad and highly interdisciplinary field which requires process engineering, material science and chemistry and provides an impressive range of functions (36). Membranes have been exploited in microfluidics in many areas, such as cell based studies, microreaction technology, fuel cells. Membrane as a novel method of microchip preconcentration-- has been a topic of increasing interest and has been intensely investigated over the last 10 years. A lot of effort has been put to the increase in functionality of microfluidic devices through integration of membranes into microfluidic networks. Khandurin et al. reported a microfabircated porous membrane structure that enables electrokinetic concentration of DNA and proteins using homogeneous buffer conditions followed by injection into a channel for electrophoretic analysis (37-39). Monolithic porous polymers prepared by photoinitiated polymerization within the channels were incorporated into a microfluidic device for on-chip solid-phase extraction and preconcentration (40). Ikuta et al. demonstrated a microconcentration chip using an ultrafiltration membrane to retain the reactive molecules. The biochemical luminescence of the process was monitored by an optical sensor (41).

1.1.3.2 Basics of Membrane Technology

A membrane can be defined as a semi-permeable barrier. It is used to control transport of some kind of species. Transport across a membrane takes place when a driving force, i.e. a chemical potential difference or an electrical potential difference, acts on the individual components in the system. There are various methods to result in the potential difference and to enable components to penetrate a membrane. Examples of these processes are the applications of high pressure, the maintenance of a concentration gradient on both sides of the membrane, a gradient in temperature and the introduction of an electric potential difference.

Membranes can be categorized from different points of view (36). One way is by membrane morphology or structure, which determines strongly the mechanisms for transport and hence the application. According to morphology, membranes can be

divided into two typical ones—open porous membranes and dense nonporous membranes.

Dense nonporous membranes, in which the choice of the material directly determines the membrane performance, can be applied in dialysis, gas separation and pervaporation. The solution-diffusion model can be used to describe transport in the systems. Basically, the transport of a gas, vapor or liquid through a dense, nonporous membrane can be described by the following equation.

Permeability (P) = Diffusivity (D) × Solubility(S)

Since solubility and diffusivity of a component are determined by its interactions with the membrane material, permeability and transport depend on the material. Selectivity for two components ($\alpha_{i,j}$), defined as the ratio of the pure permeability of components of i and j, shows the separation efficiency of the membrane.

But for open porous membranes, pore size and pore size distribution, tortuosity (τ) and surface- and volume porosity (ε) are the main factors which determine the separation characteristics and dominate transport because transport takes place through the pores instead of the material itself. Pore size is within the range of 2nm to 10μm. Different pore geometries such as cylindrical and round exist. Porous membrane media has a large surface-to-volume ratio. The membrane separation process is based on the porous structure. A very large surface area, at least 200cm^2 of internal surface per cm^2 of frontal surface can be obtained for protein absorption and immobilization. The large surface area-to-volume ratio membrane is vital because it serves to achieve fast exchange of solutions and filtration of analytes based on their different sizes. Microfiltration and ultrafiltration are their major applications. Different transport models have been proposed. One is the friction model, which considers that passage through a porous membrane occurs by viscous flow and diffusion. The term-retention(R) is used as an alternative to selectivity for nonporous membrane. Retention is given by the following formula and related to the concentration of the component in permeate and feed.

$R_i = 1 - (c_{i,perm}/c_{i,feed})$

The ratio of molecular size to pore size determines retention. For a highly selective membrane, this term must be as high as possible. It varies between 0 and 1. The value of 1 means the component is totally retained, while no retention occurs

when the number is zero. Molecular weight cut-off (MWCO) is another characteristic of a porous membrane to indicate the pore size and separation efficiency. It is defined as the molecular weight at which 90% is retained by the membrane. Combination of MWCO and permeability which is the material-dependent term can be used to evaluate the separation performance of a membrane.

Two modes are used to operate membrane (42). The first one is "dead end mode", in which a feed stream is completely passed through the membrane. Components rejected by the membrane accumulate at the membrane surface. The second one is the continuous mode, in which the feed flows along the membrane. The feed stream is divided into two streams, i.e. into the retentate or concentrate stream. The stream that is transported through the membrane is called permeates while the remainder is 'retentate'. Either one can be desired depending on the application. In the case of concentration, the retentate usually is the product. In regard to purification, both the retentate and the permeate can be the product.

1.1.3.3 Methods of Incorporation of Membranes in Microfluidic Devices

A large amount of effort has been attempted to integrate membranes and microfluidic devices. Many fabrication methods have been investigated and reported. Jong et al has roughly divided the methods into 4 types (42). A simple one is to choose a material of a microfluidic device that itself owns the membrane properties. Polydimethylsiloxane (PDMS) is the material that has won the most interest. It has very interesting properties and has been applied for over 20 years in membrane technology such as in nanofiltration(43) and pervaporation(44). In all the applications, the property of the high gas permeability of PDMS has been extensively studied and a lot of knowledge is ready to access. Although PDMS is relatively new to microfluidics, much work has been done for its high gas permeability (45-47). Other advantages of PDMS, including good optical transparency, moldability, nontoxicity and low curing temperature also contribute to its extensive usage in the fabrication of microfluidic devices (48, 49). In microfluidics, supply of oxygen or removal of carbon dioxide, particularly in cell related research is the main application of the high permeability property of PDMS. Other polymers such as polyimides (50) and cellulose acetate (51) can also be utilized.

The second method of integration of membranes on microfluidic devices is to combine commercial membranes with microfluidic devices directly. Commercially

purchased membranes are flexible, mechanically robust and compatible with plastic microfluidic devices (52). Clamping or gluing is the common and simple way to achieve the incorporation of membranes with microfluidic devices. Some modification of membranes may be made (53, 54).

Preparation of a membrane in the process of fabrication of a microfluidic device is the third approach. Some technology of semiconductor industry or integration of semiconductor technology and some polymer techniques (55, 56) have been applied. Many fabrication approaches such as etching (57), film deposition (58) and porous layers formed from zeolite (59), silicon (60) et al. have been demonstrated.

The last strategy is to prepare a membrane on an already existing format of a microfluidic device. Different ways of polymerization *in situ* have been reported, such as emulsion photo polymerization (61), laser-induced phase separation polymerization (62, 63) and interfacial polymerization (64). In addition, formation of liquid layer membranes in a microfluidic device has been reported (65).

The first method of utilizing the material property is simple and elegant and it doesn't need additional preparation steps for membranes. The advantages of direct integration of commercial membranes with a microfluidic device are the simplicity of the fabrication steps and the broad selection range of commercial membranes according to their applications. With a standardized design of a microfluidic device, simply changing the type of a membrane can meet different demands (42). But it has the problem in the sealing step that capillary forces can suck glue into the membrane pores and lead to the blocking of the membrane. For the third approach, membrane preparation in the process of fabrication of a microfluidic device, it bears the advantages of good control of feature sizes and chemical/thermal resistance of used materials. But the process by semiconductor technology is very complex and consumes a lot of money and labor. Laser-induced phase separation in situ polymerization opens the possibility to control the position and thickness of the membrane. The difficulty of developing a liquid membrane in a microfluidic device lies in the difficulty in obtaining a stable interface and the limited knowledge in this field.

1.1.3.4 Applications of Membranes in Microfluidics

Many reviews of applications of membrane methods in the field of analytical chemistry have been published (66-71). The papers were based on the general

experience that was obtained in chemical analysis by using membranes. With the rapid emerging of microfluidic technology in analytical chemistry and the expansion of membrane methods into microfluidics, some review papers (42, 52, 72, 73) about applications of membranes in microfluidics have been published. The review (42) provides the overall developments of this field including basics of membrane technique, methods of membrane integration with microfluidic devices, applications, discussion of considerations for the use of membranes and a checklist with selection criteria, with the aim to build a bridge between membrane technology and microfabrication. It has exhibited both traditional and new usages of membranes in the area of microfluidics, such as sample concentration, filtration, and preparation, gateable interconnects and gas sensors. Applications in some new fields such as membranes microreactors cell related research and fuel cells are also available. Bioanalytical applications of incorporation of membranes into microfluidic network have specifically been focused in the review paper (52). The work summarized in this paper mainly covers those employing commercial membranes in microfluidic devices. The range of the bioanalysis in this paper includes microdialysis sample cleanup and fractionation, affinity microdialysis/ultrafiltration, protein digestion, membrane chromatography (reversed-phase separation and chiral separation). It is pointed out that the commercial membranes are able to offer fast microdialysis for sample cleanup and fractionation in microfluidic devices and high throughput residue analysis of food contaminants and drug screening of small-molecule libraries is achievable. An extraordinary solid support for protein adsorption and immobilization is also performed by the membranes. The review paper (72) has discussed sample pretreatment in the use of membranes in microfluidic devices in addition to comparisons with other methods such as extraction and electrohporesis. Perterson (73) has examined different methods of incorporation of solid supports into microfluidic devices and compared membranes with beads, gels and monoliths. It is indicated that integration of membranes into microfluidic devices is very simple; although it bears the limitation that the limited volume of membranes might prohibit their applicability within a few applications.

There are some challenges that might be encountered when combining membrane technology with microfluidics (42).For example, one problem is concentration polarization which is resulted from the fact that a solvent from a solution through a membrane is removed faster than the transport of the new solvent

from the bulk to the membrane surface. As a result, the concentration of a solute in the local membrane increases and the driving force over the membrane decreases. In addition, the concentration polarization might also cause fouling and/or scaling of the membrane.

All in all, the combination of membrane technology with microfluidics is getting stronger every day and the future for combination of the both fields looks bright (42). Applications of membranes to microfluidics have been demonstrated in separation and phase contacting. There are still a lot of opportunities that are waiting to be explored, such as the selectivity of dense nonporous membranes, bipolar membranes which is composed of a positively and a negatively charged membranes, with a catalyst in between (74).

The sol-gel process is one of the most suitable methods for the preparation of membranes. Membranes which are fabricated using sol-gel chemistry have several advantages over traditional organic polymer membranes (75): they can be used at high temperature; they do not swell or shrink when they are in contact with water and they resist abrasion very well. Sol-gel membranes were fabricated inside glass chips in this work. In next section, sol-gel chemistry and the sol-gel process will be discussed for making membranes.

1.1.4 Application of Sol-Gel Chemistry to Membrane

1.1.4.1 Sol-gel process

Since the late 1970's, the development of sol-gel materials has been increasing. Sol-gel technology, which has the advantages of the ease of preparation, modification and processing of the materials along with their high optical quality, photochemical and electrochemical inertness and good mechanical and chemical stability, is a powerful tool for the fabrication of inorganic and inorganic-organic hybrid materials including membranes (76, 77). Inorganic-organic hybrid materials such as organically modified silicates (ORMOSILs) offer properties better than those prepared alone. Many configurations such as monoliths, fibers, thin and thick films can be achieved in the process of fabrication. Sol-gel materials have been applied in many fields, such as membranes, chemical sensors and catalysis (78).

The term sol-gel originates from the individual terms of sol and gel. A sol is a suspension of solid particles in a liquid. The size of the dispersed phase (solid particles) is very small (between 1-1000nm) and thus gravitational forces are negligible and interaction is dominated by short-range forces like van de Waals attraction and surface charges (79). The small solid particles are typically metal oxides or metal alkoxides and they are also called precursors in the sol-gel process. The precursors of the sol undergo polymerization which leads to the growth of clusters that finally collide and link together into a gel.

A sol-gel process usually involves catalytic hydrolysis of sol-gel precursor(s) and catalytic polycondensation of the hydrolyzed products and other sol-gel-active components present in the reaction medium to form a macromolecular network structure of sol-gel materials (80-81). Any sol-gel material is formed through 4 steps. The first one is hydrolysis and condensation in which precursors or monomers such as metal oxides or metal alkoxides are mixed with water and then undergo hydrolysis and condensation to form a porous interconnected cluster structure. An alcohol is chosen as a solvent for the precursors since they are often insoluble in water. Either an acid such as HCl or a base like NH_3 can be employed as a catalyst.

The second step is gelation. As the first step of hydrolysis and condensation continues, more particles join the clusters. The clusters grow bigger and bigger and then collide each other and link together to generate a single giant spanning cluster which is called gel. With time, more clusters present in the sol phase will become connected to the network and the gel will become stiffer and an increase in viscosity and elasticity will result in. In addition, hydrolysis and condensation do not stop with gelation. They continue to pass gelation and go to the next step of the sol-gel process.

Aging is the third step of the sol-gel process. During aging, the process of change after gelation can be divided into polymerization, coarsening and phase transformation (79). Because of presence of the unreacted hydrolysis groups, condensation reactions continue, resulting in the increase in connectivity of the network and thus the increase in stiffness and strength of the gel. As the continuing condensation process go on, the pores of the gel will become smaller and liquid in the

pores will be expelled, leading to gel shrinkage or syneresis. Another change in the process of aging is coarsening, also called ripening. This process involves dissolution and reprecipitation which is driven by differences in solubility between surfaces with different radii of curvature. The smaller particles, which have positive radii of curvature and higher solubility, dissolve again and precipitate into crevices and necks between particles, which have negative radii and lower solubility allowing material to accumulate there. This serves to increase pore size, by filling in smaller pores, and strengthen the network (82). In addition, phase transformation may take place during aging, such as crystallization from amorphous structure, segregation of a liquid phase into two or more phases.

Drying is the last step of the sol-gel process. It can be divided into three stages. In the first stage, due to evaporation of the liquid in the pores, the gel shrinks. The gel network experiences deformation thanks to capillary forces. New connections in the network are also formed and continue to strengthen the network (82, 83). The liquid-vapor interface remains at the external surface of the gel. Shrinkage continues until stage two starts (84). The second stage starts when the gel becomes too stiff to shrink and reaches the critical point in which the capillary forces are the highest and the pores begin to empty the liquid in them. At this point, liquid evaporation from pores is slowing down (85). The liquid recedes into the interior, leaving air-filled pores near the surface (86). Finally, once the liquid is primarily out of the pores, the liquid is isolated into pockets. Evaporating within the gel body and diffusing the vapor to the exterior is the only way for remaining liquid. No further shrinkage occurs. Loss of weight is the only significant change until equilibrium is reached with the environment (82).

Sol-gel process has the ability to control the properties of the matrix by choosing different parameters for processing. A large variety of compounds (e.g., semiconductor, biomolecules, organometallics, and even small organisms) can be integrated into the sol-gel matrix to obtain sol-gel materials with different properties (87-90). Factors that influence the structure and properties of sol-gel materials will be covered in the following section.

14

1.1.4.2 Factors Affecting the Structure and Properties of Sol-gel Materials

Although all sol-gel materials form by following the same 4 basic steps, the properties and structures of the materials produced are quite different. The chemical reactions during the four steps in the two routes have a great effect on the composition and properties of the final sol-gel material (91, 92). Sols and gels evolve in different ways when different types of precursors are used. For example, the size of the alkoxide group dictates the rates of hydrolysis and condensation due to steric effects. The large alkoxide groups result in the slow hydrolysis rate and a high extent of branching. For the case of the precursors of organically modified silanes (ORMOSILs), it is even more complicated. The relative rate of hydrolysis and condensation strongly depends on steric and inductive factors. The sol-gel process is even more complex when the organic functional group contains acidic or basic moieties (93). However, through careful control of hydrolysis and condensation, ORMOSILs add flexibility to the silica gel and offer specific tailoring of the sol-gel matrix, such as alteration of pore sizes and polarity, introduction of hydrophobicity and introduction a specific functional group to be covalently bound into the sol-gel matrix (91, 94).

Other sol-gel process parameters such as water-to-silane ratio and the nature and concentration of the catalyst also strongly affect the relative rates of hydrolysis and condensation which, in turn, dominate the physical properties of the sol-gel materials (i.e., surface area, average pore size and distribution) (95). Under acid catalysis, condensation happens preferentially between silanol groups on monomers and the ends of polymer, resulting in formation of long chains mainly and a lower pore volume matrix, while highly branched particulate gels and materials with higher interstitial porosity after drying are generated with catalysts of bases. As far as the water to silane ratio (r), when r is larger, the rate of hydrolysis increases and the rate of condensation reduce. As a result, a more porous material with higher surface area will be formed. Conversely, under the condition that r is less than 4, a denser material with smaller average pore size will be obtained (80).

Sol-gel materials are also affected by drying treatment of gels. Xerogel formed by drying under ambient conditions has lower porosity than aerogel, another drying product of gels under the conditions above critical temperature and pressure where there is no capillary pressure. The latter has extremely high porosity, as high as 95% (95).

1.1.4.3 Sol-gel Chemistry and Membrane Processing

The above sol-gel steps are presented from a very general view. Actually this process can be divided into two sol-gel routes which are both able to generate porous materials (91). Colloid chemistry in aqueous media is the foundation of one route. The other route is based on the chemistry of metal organic precursors in organic solvent (91). Here how the different steps affect the porous structure of membranes for the two different routes will be stressed. Sol-gel chemistry to the two routes will be compared. More emphasis will be put on the second route since it was exploited to fabricate membranes in this work.

For the first method, the DLVO theory talks about the formation of colloidal suspensions in aqueous media. Gel formation is dominated by steric or electrolytic factors of physical gels. During this process, individual particles are arranged and surrounded by either steric barrier or an electrical double layer which is generated by acid-base reaction at the particle/water interface. The degree of aggregation of particles depends on the potential difference from the electrical double layer. Therefore, the interaction forces, determined by the pH and the nature and the concentration of the electrolyte, have a direct effect on the gel porosity. Membranes with a low porosity (30%) are generally obtained under the conditions of a strong steric effect or a high repulsion barrier between particles, while highly porous membrane materials can be achieved due to a partial aggregation of particles from a weak interaction. Usually sol-gel process of colloidal sols results in mesoporous membranes. Sintering temperature is another factor that influences the porous structure of membranes.

For the second method, organic media is used and polymeric gels are formed. The formation of polymeric gels depends on the relative rates and extents of chemical reactions, thus depends on some factors like acid or basic catalysis and precursor concentration. Sequential polymer growth in the sol generates polymeric gels which subsequently collapse and crosslink. The structure of individual clusters resulting from polymerization will determine the size and the structure of the pores. Both low-branched and high-branched clusters can be formed by adjusting the conditions of hydrolysis and condensation (96, 97). Microporous membranes, which have smaller pore size than mesoprous membranes, can be obtained through low –branched clusters resulting from polymeric sols, while high-branched clusters lead to micro or mesoporous materials due to steric hindrance.

Chemistry of colloidal sols is quite different from that of polymeric sols. Hydrolysis and condensation of metal salts in aqueous media result in the formation of colloidal particles. A metal cation will be solvated and hydrolyzed and converted to new ionic species by water molecules when dissolved in water, resulting in formation of three types of ligands: aquo ligands(OH_2), hydroxyl ligands(-OH) and oxo ligands (=O).

$$M^{Z+} + :OH_2 \rightarrow [M \leftarrow :OH_2]^{Z+}$$
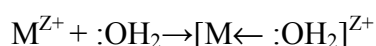
Normally, aquohydroxo and/or hydroxo complexes will be generated for low-valent metal cations ($Z < 4$), while oxo-hydroxo and/or oxo complexes will be obtained for cations of $Z > 5$. Both of the cases are over the whole range of pH. Tetravalent cations are in the middle. Therefore a large variety of possible precursors will be formed and then they will start on condensation following two mechanisms of reactions:

(1) –olation (nucleophilic substitution)

$$M\text{-}O^{\delta\text{-}}H + M^{\delta+}\text{-}O^{\delta+}H_2 \rightarrow M\text{-}OH\text{-}M + H_2O$$
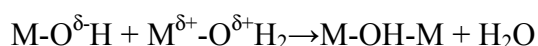
(2) –oxolation (nucleophilic addition with or without an OH leaving group)

$$M\text{-}OH + HO\text{-}M \rightarrow M\text{-}O\text{-}M + H_2O$$
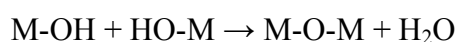
Aquo ions cannot experience condensation since no entering group is available and oxo ions can only undergo condensation via addition when the precursor is

unsaturated. Therefore it is necessary to adjust pH in order to get hydroxo complex for condensation. Normally the pH range for colloid particles to branch is within 2-8.

In polymeric sols, the hydrolysis and condensation of metal organic precursors in organic media forms the dispersed phase. Most cases are the polymerization of metal alkoxides in an alcohol with the following reactions.

(1) Hydrolysis

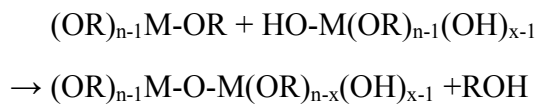$$M(OR)_n + xH_2O \rightarrow M(OR)_{n-x}(OH)_x + xROH$$

(2) Condensation

$$(OR)_{n-1}M\text{-}OR + HO\text{-}M(OR)_{n-1}(OH)_{x-1}$$

$$\rightarrow (OR)_{n-1}M\text{-}O\text{-}M(OR)_{n-x}(OH)_{x-1} + ROH$$

Or/and

$$(OH)_{x-1}(OR)_{n-1}M\text{-}OH + HO\text{-}M(OR)_{n-1}(OH)_{x-1}$$

$$\rightarrow (OH)_{x-1}(OR)_{n-1}M\text{-}O\text{-}M(OR)_{n-x}(OH)_{x-1} + H_2O$$
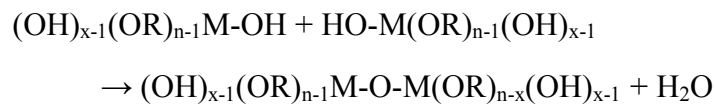
In order to fabricate microporous and ultramicroporous membranes, polymeric sols containing clusters with controlled size and low mass fractal dimension should be used. Mass fractal dimension (D) indicates the relationship between the cluster mass and its radius by $M \propto r_c^D$. When D is less than 1.5, the intersection of two mass fractal objects decreases as r_c increases, which can lead to increased interpenetration of clusters and an very fine texture of microporosity. There are some methods and strategies available for the control of hydrolysis with transition metal alkoxides in literatures (98-100). Membranes with pore size down to the nanometer range can be produced using sol-gel chemistry.

In this work, titanium isopropoxide — a transition metal alkoxide was used as the sol-gel presursor to synthesize sols for formation of microporous membranes on a glass microfluidic chip. The detailed procedure of fabrication will be given in the experimental section.

1.1.5 Fundamentals of Fluorescence Detection

Laser-induced fluorescence detection is an extremely sensitive detection method. Table 1.1 compares some common detection methods (101). It can be seen clearly that both the mass detection limit (moles) and the concentration detection limit (Molar) of laser-induced fluorescence are among the lowest range, which allowing it to be applied in many fields, such as chromatography, flow cytometry, electrophoresis and DNA sequencing. A fluorophore is a functional group of a molecule (often polyaromatic compounds) which can cause a molecule to be fluorescent by absorbing energy of a specific wavelength and emitting energy at another wavelength. Fluorescence occurs when a fluorophore molecule or quantum dot relaxes to its ground state (S_0) after it is electronically excited to a state with higher energy, such as the first excited state (S_1):

Excitation: $S_0 + h\nu \rightarrow S_1$

Emission: $S_1 \rightarrow S_0 + h\nu$
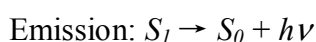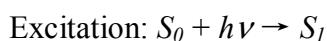
A photon with energy of $h\nu$ of a different wavelength from that of the absorbed energy is produced in the process of emission. The excited state electron exists for about 1-10ns and then back to the ground state by various competing pathways, such as fluorescence, phosphorescence via a triplet state, non-radiative relaxation (heat release via vibration). The energy difference between the excited state and the ground state yield stokes shift, which allows for the separation of excitation light from emission light through bandpass or holographic notch filters. Therefore low background and high signal to noise ratio can be obtained for detection. Autofluorescence, photobleaching and some other factors also have an important influence on sensitivity of LIF detection.

Several methods are available to attach a fluorophore to a non-fluorescent molecule interest to generate a new and fluorescent molecule. The most common way is to chemically link a fluorophore through organic reactions with primary amines, thiols or alcohols. Amine derivitization is generally employed to modify proteins, ligands and peptides for immunochemistry, cell analysis, fluorescence in situ labeling, while thiol derivitization is used to investigate protein function and structure.

Three types of reagents are commonly used to activate a fluorophore. They are isothiocyanates, succinimidyl esters (SE) and sulfonyl chlorides. Fluorescin isothiocanate, a reactive derivative of fluorescein, was used in this work. It is one of

19

the most common fluorephores that can be chemically attached to other non-fuorescent molecules to generate new and fluorescent molecules. Other common fluorophores are derivatives of rhodamine, and coumarin. A newer generation of fluorophores such as the Alexa Fluors and the Dylight Fluors has been synthesized with the advantages of higher-photostability, less pH-sensitivity and et al.

Table 1.1 Different methods of detection

Detection methods	Mass detection limit (moles)	Concentration detection limit (molar)	Advantages/disadvantages
UV-Vis absorption	10^{-13}-10^{-16}	10^{-5}-10^{-8}	Universal; Diode array offers spectral information
Fluorescence	10^{-15}-10^{-17}	10^{-7}-10^{-9}	Sensitive; Usually requires sample derivatization
Laser-induced fluorescence	10^{-18}-10^{-20}	10^{-14}-10^{-16}	Extremely sensitive; Usually requires sample derivatization; Expensive
Amperometry	10^{-18}-10^{-19}	10^{-10}-10^{-11}	Sensitive; Selective but useful only for electroactive analytes; Requires special electronics and capillary modification
Conductivity	10^{-15}-10^{-16}	10^{-7}-10^{-8}	Universal; Requries special electronics and capillary modification
Mass spectrometry	10^{-16}-10^{-17}	10^{-8}-10^{-9}	Sensitive and offers structural information; Interface between CE and MS complicated

1.2 Experimental

1.2.1 Reagents

Titanium isopropoxide was obtained from Gelest (Morrisville, PA) and kept in a dissicator at room temperature. Sodium phosphate and 2-propanol were purchased from Acros Organics (Geel, Belgium). Arginine (Arg) was bought from INC Biomedicals Inc.(Aurora, OH). Fluorescein isothiocyanate (FITC) was obtained from Molecular Probes (Eugene, OR). Acetone, methanol and dimethylsulfoxide(DMSO) were got from Fisher (Pittsburg, PA). Chrome Mask Etchant was purchased from Transene, Co. (Danvers, MA). All the solutions were made with distilled, deionized water from a Barnstead Nanopure System (Dubuque, IA) and then filtered by 0.45μm Acrodiscs (Gelman Sciences, Ann Arbor, MI). All the chemicals were used as received.

1.2.2 Fluorescent Derivatization

A 10mM stock solution of FITC was prepared in DMSO. A 5mM stock solution of arginine was made in 150mM sodium bicarbonate solution (pH=9) and mixed very well (check the pH of the 150mM solution of sodium bicarbonate and make sure it is at 9 before use, because FITC wouldn't react very well with amino acids under pH of 9). Add 900μL the arginine solution to 100μL the FITC solution and then place it on a shaker in dark for 4 hours at room temperature. After 4 hours, the stock solution is stored in the freezer until needed. All solutions were made using distilled deionized water from a Barnstead Ultrapure Water System (Dubuque, IA) and filtered with 0.45μm Millex®-LCR syringe driven filter units(Millipore Corporation; Bedford, MA). The labeled arginine stock solution was diluted to different concentrations in an 80mM sodium phosphate solution at pH 11.5.

1.2.3 Glass Microchip Design and Fabrication

1.2.3.1 Design

Fig 1 shows the scheme of the glass microchip design with a cross –shape and four reservoirs used in this work. The dimensions for some channels were listed in the diagram.

21
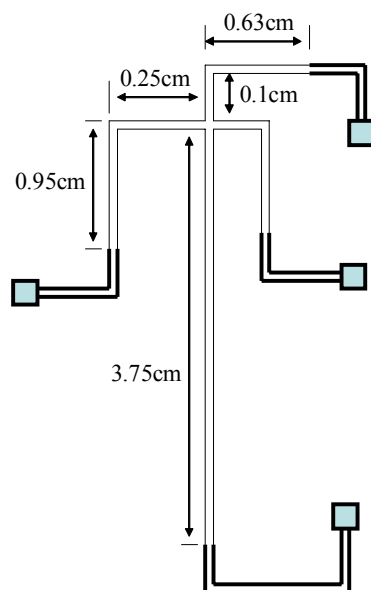
Figure 1.1 Diagram of the glass microchip design

The autoCAD LT 2002 program from Thompson Learning (Albany, NY) was employed to create the design. The drawing of the design was sent to the photomask fabricators (Colorado Springs, CO) for translation and fabrication. The channels were typically 10μm in height and 50μm in width at half-height.

1.2.3.2 Materials and Instruments

The e-beam written chrome mask was obtained from Advance Reproductions Corporation (Andover, MA) and used to pattern the photomask blanks which were purchased from Telic Co.(Santa Monica, CA). The photomask blanks was coated with chrome and AZT positive tone photoresist and have the dimensions of length of 10.16cm, width of 10.16cm and height of 0.16cm. A flood exposure system was obtained from ThermoOriel (Straford, CT). A Micriposit Developer solution was purchased from Shipley Co. (Marlborough, MA). A solution of Chrome Mask Etchant and a buffered oxide etchant were obtained from Transene, Co.(Danvers, MA). The buffered oxide etchant, which was composed of NH4F and HF with a ratio of 10 over 1, was mixed with water and HCl with a volumetric ratio of 1/4/2. A hydrolysis solution was made in house using NH_4OH, H_2O_2, and H_2O with a proportion of 1:1:2.

Epo-tek 353ND Epoxy was purchased from Epoxy Technologies, Inc. (Billerica, MA). Cover plates were obtained from Technical Glass Inc. (Aurora, CO).

A stylus-based surface profiler (Ambios Technology; Santa Cruz, CA) was used to determine the channel dimensions. A dicing and cutting saw from MTI Corp., USA was used to cut the glass substrate and a cover plate.

1.2.3.3 Procedure of Fabrication and Bonding

The standard photolithographic process and chemical wet etching used to form the channels are briefly described as follows. The photoblank slide (glass substrate) was exposed to UV light for 4s at a power of around $45\mu J\ cm^{-2}$. The exposed plate was immersed into the solution of Microposit Developer for 1.5min and washed completely with distilled water. Subsequently it was placed in the Chrome Mask Etchant for 3min and rinsed with water and dried using nitrogen gas. Then the exposed glass was put into the buffered oxide etching solution for chemical wet etching for around 8 min. During the etching process, the height of the channels was checked using the profiler. Once the height reached the desired $10\mu m$, the slide was rinsed thoroughly using acetone, ethanol and water in order and dried with N_2. After making a marker on each slide with a design of the plate, the slide has reimmersed the slide back into the Chrome Mask Etchant solution for 10 min to remove the remaining chrome and wash and dry it completely. Then the glass substrate was cut into 8 pieces of slides by using the dicing and cutting saw, each with a dimension of 2.54 cm×5.08 cm. A cover plate with holes was cut in a same way with the same dimension. Then 8 pieces of top slides were obtained.

The channels on the glass substrate slide were enclosed by bonding the substrate slide to a piece of cover plate. Briefly, first, the slides stayed in a stirred solution of 5M sulfuric acid for 5min. Second, the slides were sonicated in a soap solution, and then in acetone for 15min each. Then they were then placed in the buffered oxide etching solution for 15sec. Next, they were immersed in the stirred hydrolysis solution for 12 min at 60℃ and sonicated in flowing distilled water for 60s prior to bonding. Between each step, the slides were thoroughly rinsed with water to ensure they were clean and dried to make sure they wouldn't contaminate the next solution. When starting bonding, the etched slides were removed at one time under the flowing distilled water and were put on Cleanroom Wipers with the etched sides

facing up. Then cover slides were removed and placed on the top of the etched slides. Binder chips were fastened on the perimeter of the slides to make sure the two surfaces contact each other. Vacuum was applied to drive out water from the channels as much as possible. And then the slides were put in an oven at 95℃ for 15 min to remove the remaining water and annealed at 565℃ for bonding the two slides together. In the end, cylindrical glass reservoirs with around 140μL volume were affixed to the access holes on the cover plate using the epoxy. The glass microchips are ready to use.

1.2.4 Fabrication of Nanoporous Membranes
1. 2.4.1 Fabrication Conditions

As discussed previously, the water to silane ratio (r) has a great influence on the structure of the resulted silane sol-gel materials. When using a higher r, the rate of hydrolysis increases and the rate of condensation decreases, resulting in a material with a higher porosity and a larger surface-to-volume ratio. Since the reactivity of transition metal oxide with water is higher than that of silane, a solution of 25% (v/v) titanium isopropoxide in the solvent of isopropanol was used for the precursor. Another solution of water in isopropanol with volumetric concentration between 10-90% was employed. The concentration of water in this sol-gel reaction plays a key role in obtaining the desired width of the membrane. In the glass microchips, laminar flow of solutions driven by pressure was exploited to fabricate titanium membranes. The membranes with widths of 4-26μm, lengths of 15- 500μm and depths of 20μm can be obtained. The range of membrane widths of 4-26μm has a linear relationship with the concentration range of water between 10-90%. A concentration of water with 50% (v/v) was finally chosen for constructing titanium membranes for sample preconcentration in this experiment. Flow rates of the two solutions, reaction times, temperature and other factors that might affect the fabrication process were kept constant. The absolute driven pressure was held at around 85KPa. The sol-gel reactions were allowed to proceed for 5min. The whole process was carried out at room temperature of about 23℃. The ambient relative humidity was around 20%.

1.2.4.2 Fabrication Procedure

(1) Clean step: Neat isopropanol was filled into the reservoirs and sucked through the channels out by applying vacuum to get rid of dust that might be trapped in the reservoirs.

Neat isopropanol was run through the channels for 5 min by applying a vacuum pressure to remove any unwanted stuff that might be trapped in the channels.

(2) Laminar flow was established by using vacuum pumps to apply pressures to the left and bottom reservoirs.

(3) The interface between the two flow solutions was checked under a microscope using two different solvents with different refractive indices (e.g. isopropanol and methanol) to ensure the sol-gel reactions would take place at the cross section.

(4) As indicated in Fig 1.2, once the check on the interface was achieved, the solvent in the top reservoir was replaced by adding the 25% solution of titianium isoproxide in isopropanol; and the solvent in the reservoir on the right was replaced by the 50% solution of water in isopropanol. This step was carried out very quickly to ensure a success fabrication of a membrane. The two reactive solutions were allowed to react for 5 min at the cross section of the glass chip.
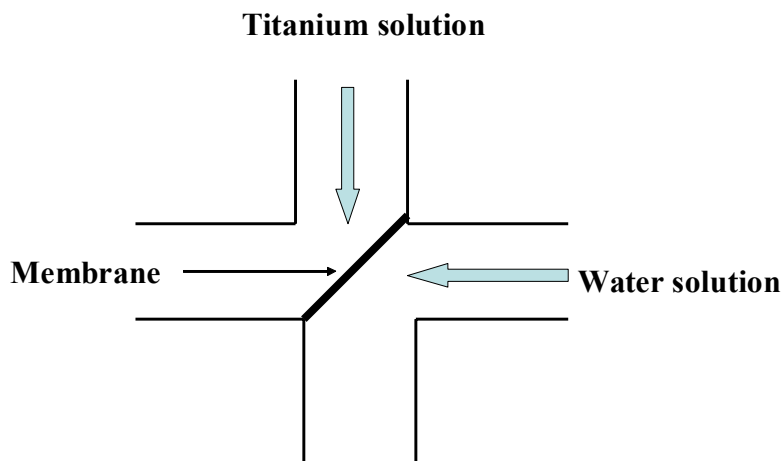
Figure 1.2 Diagram of membrane fabrication on a glass chip

(5) The two solutions were removed from the two reservoirs and the two reservoirs were rinsed thoroughly with neat dry isopropanol replaced with neat dry isopropanol. Then the channels were rinsed by running isopropanol through for 3 min.

(6) An 80mM phosphate buffer solution with a pH of 11.5 was added to take the place of isopropanol and then was run through the channels for 3min.

(7) Vacuum pumps were removed from the reservoirs at the same time and the phosphate buffer was filled into the other two reservoirs.

(8) The membrane in the glass chip was kept 24 hours at room temperature in a clean environment before it was ready to use.

1.2.5 Instrumentation

A custom-built high voltage power supply with five individual outputs was used to control the process of sample preconcentration and separation. Platinum electrodes were used to apply voltages to solutions in the reservoirs. A single-point laser-induced fluorescence detection setup using an argon ion laser (488nm) was employed to monitor separation performance. Imaging was taken by using a Nikon Eclipse TE 2000E microscope with an attached scientific grade CCD camera (Princeton Instrument's MicroMax; Roper Scientific, Trenton, NJ). Control of voltage outputs and relays and data acquisition were made using computer programs written in LabView (National Instruments, Austin, TX).
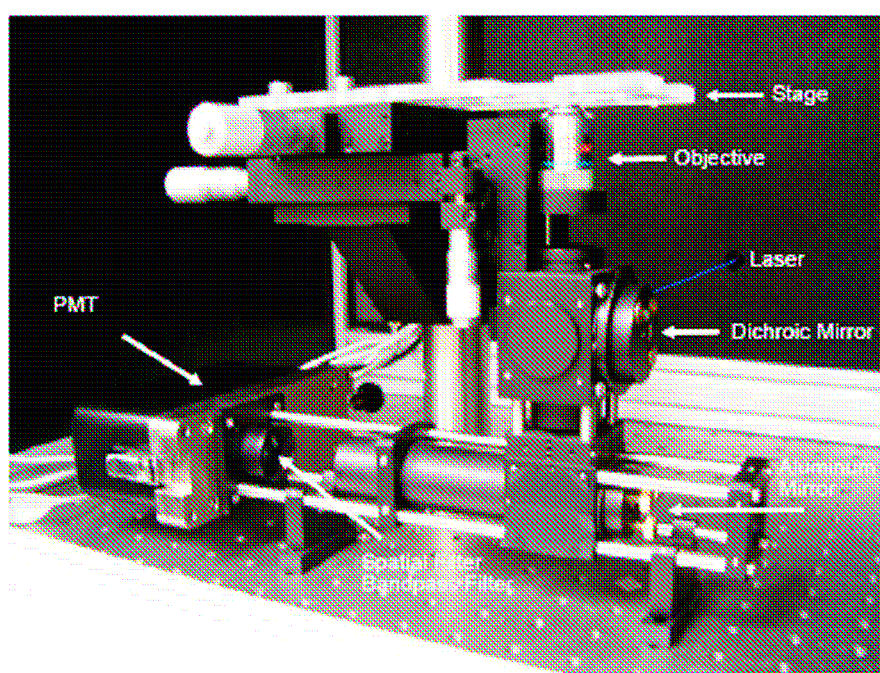

Figure 1.3 Single point apparatus for laser-induced fluorescence detection

The home-made single point setup for fluorescence detection exploits an argon ion laser (35-MAP-431-208; Carlsbad, California) as the excitation light, which has the ability of producing 70mW laser lines at 488 nm and 514nm. The laser lines were reflected off a 500 (or 560) nm long-pass dichroic mirror (500DRLP or 560DRLP) (Omega Optical; Brattleboro, VT) and focused by a 40X objective (CD-240-M40X; Creative Devices; Mechanic Station, NJ) into a small spot in a separation channel. The excitation light from the fluorophore was collected by the same objective, transmitted through the dichroic mirror and then spatially filtered using a 1mm pinhole (Oriel, Stratford, CT) and spectrally filtered by a bandpass filter(545 AF 75 or 595 AF 60; Omega Optical). A photomultiplier tube (PMT, R1477; Hamanatsu Instruments, Inc.; Bridgewater, NJ) was used to detect and an SR 570 low noise current preamplifier (Stanford Research Systems, Inc.; Sunnyvale, CA) with a 100HZ lowpass filter was employed to amplify the signal which was subsequently sampled at 200Hz using a PCI-6036E multifunction I/O card (National Instruments, Inc.; Austin, TX) in a computer. The program of Igor Pro of Labview was used to analyze all the data for sample detection.

The optical parts such as bandpass filters and dichroic mirrors play very important role in the sensitivity of the detection. Dichroic mirrors act as a beamsplitter and are capable to reflect and transmit light by utilizing a large number of coating techniques. They are used to transmit specific range of wavelengths through the filter and reflect other range of wavelengths to obtain the desired wavelengths for detection.

1.3 Results and Discussion

Silica membranes using sol-gel processing were already exploited on microfluidic devices with different designs for sample preconcentration by Ramsey (37-39). The formation of the silica membranes was accomplished in the process of fabrication of the microchips. Photolithography and chemical wet etching were used to transfer the microchip design onto the glass substrate. The bonding step of the glass substrate and the cover plate was quite different from that in this work. A low-temperature bonding process using a spin-on silicate adhesive layer as the adhesive was applied to bond the cover plate and the glass substrate and form the enclosed network of channels. Briefly, a silicate solution (usually potassium silicate) was

diluted with deionized water and then spin-coated onto the cover plate. Subsequently the treated cover plate surface was brought into contact with the etched glass substrate surface immediately. In this process, a narrow layer of porous silica membrane was formed because of polycondensation of the silica sol-gel reaction and served as the adhesive to connect the two surfaces. And then the bonded assembly was annealed at 200℃, which was utilized to strengthen the bonding through dehydration and siloxane bond formation. The resulted semipermeable silica membranes, serving as a filter, allowed passage of ionic current but blocked large molecules in this microchip design, Therefore, it enabled and demonstrated preconcentration of protein and DNA samples to achieve good separation and detection performance, as shown in the papers.

In our work, the purpose was to check on the function of a porous membrane formed *in situ* in glass microchips with the different design (as indicated in Fig 1.1) using a different sol-gel precursor of titanium metal alkoxide.
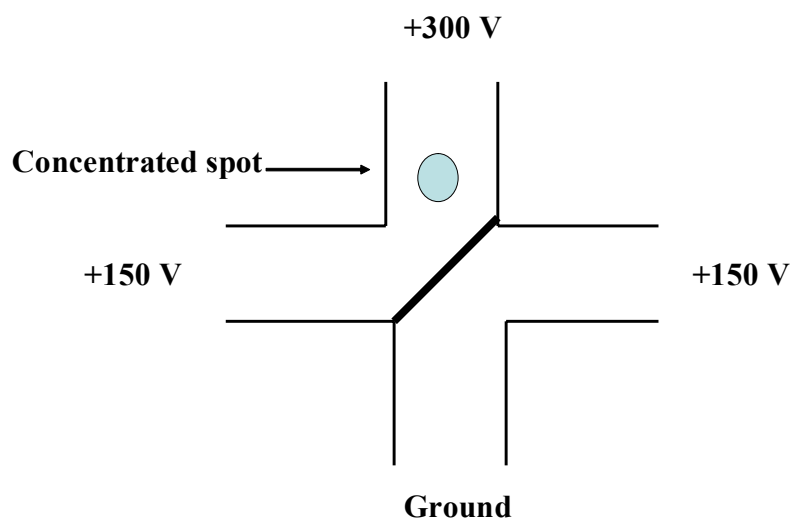
Figure 1.4 Schematic of membrane concentration on a glass chip

Fig 1.4 shows a schematic diagram of preconcentration. A high potential of 300 V was applied to the top reservoir. A potential of 150 V was applied to the two side reservoirs individually which was used to prevent bleeding of the excess sample into the separation channel (the side channel to the right as indicated in Fig 1.5) in the process of preconcentration. The bottom reservoir was connected to the ground. The nanoporous property of the membrane combined with this voltage scheme allows

28

small buffer ions to pass through the porous membrane while prohibiting the passage of large molecules. Therefore, large molecules can be accumulated at the top channel, as indicated by the light blue spot.

Fig 1.5 presents preconcentration images for samples with different concentrations taken by CCD camera using Winview 32 software. It can be seen clearly that preconcentration effect was able to be achieved down to samples of picomolar concentration. Fig 1.5 (d) depicts the image for a FITC-labeled amino acid of arginine with a nanomolar concentration. Occasionally leakage of the concentrated plug into the separation channel was observed. It might be due to imperfect fabrication or breakdown of the membrane by applying the high potential difference on the two sides of the membrane.
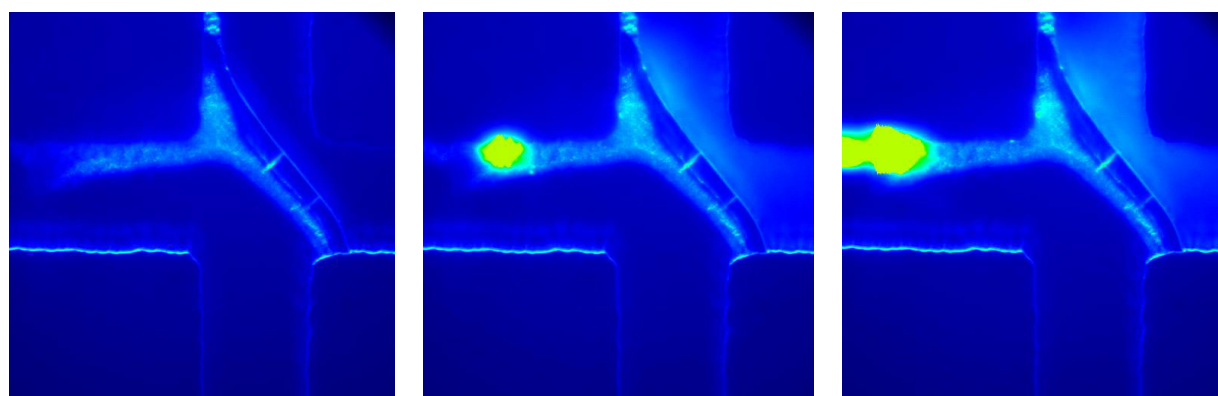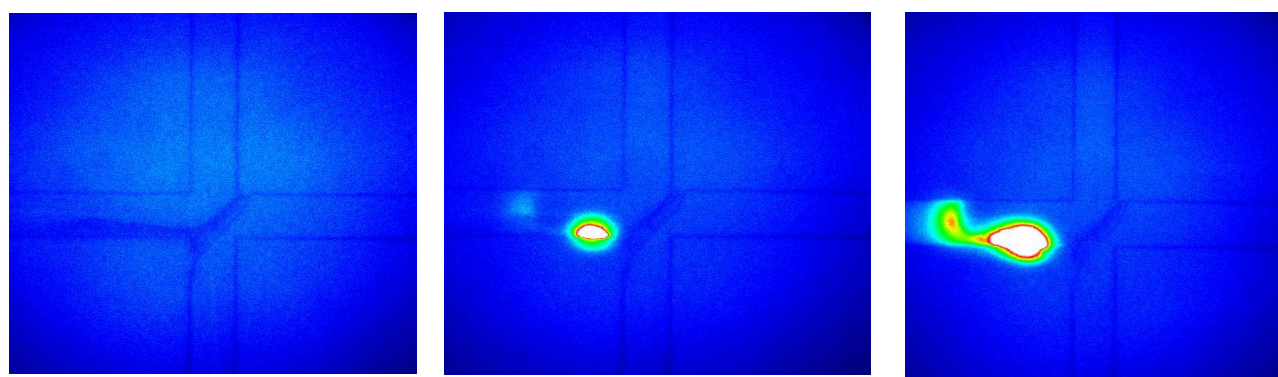

| 0 min | 5 min | 10 min |

(a) Images for 0.3μM Standard fluorescein sample concentrated plug
(P.S. the different membrane position was because the mask was put upside down during fabrication of the glass chip, which didn't affect its usage.)
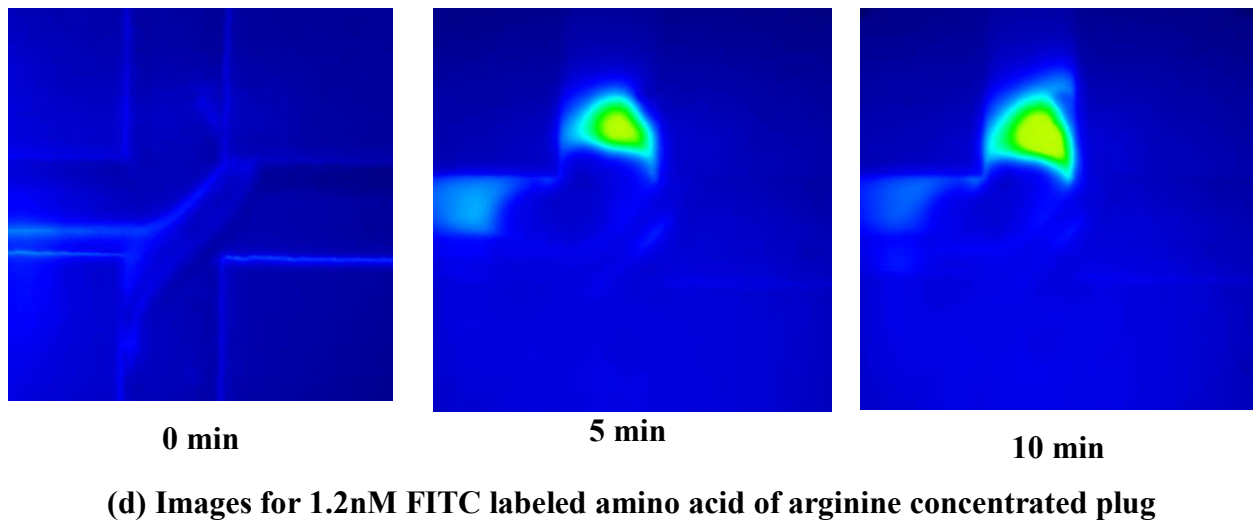

| 0 min | 5 min | 10 min |

(b) Images for 1.36nM standard fluorescein sample concentrated plug

0 min	**5 min**	**10 min**

(c) Images for 3.2pM standard fluorescein concentrated sample plug

0 min	**5 min**	**10 min**

(d) Images for 1.2nM FITC labeled amino acid of arginine concentrated plug
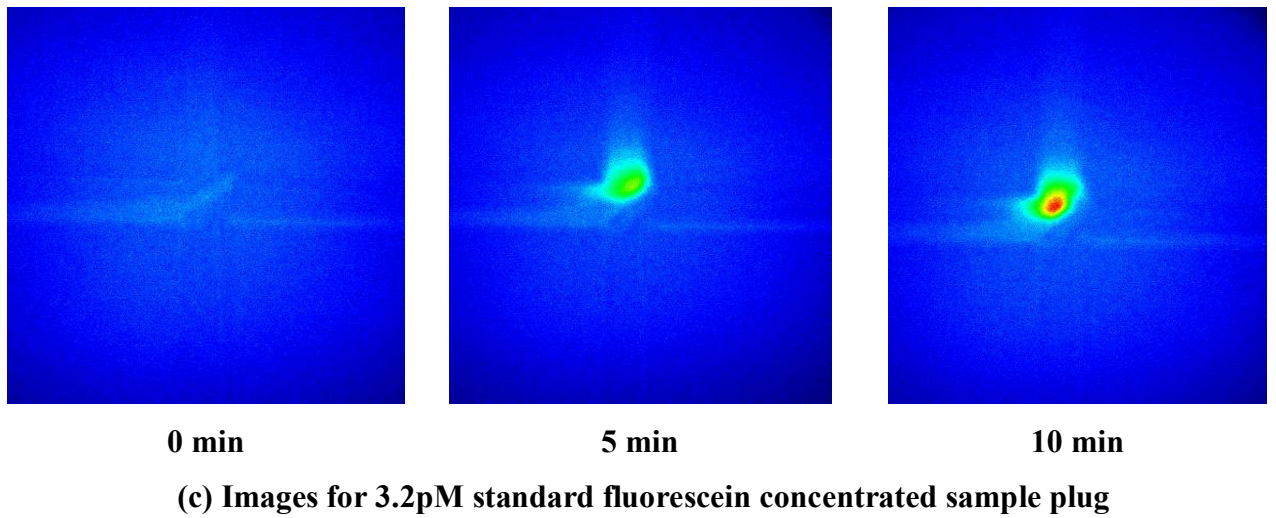
Figure 1.5 Images of concentrated plugs for different samples generated by membranes on glass chips: (a) 0.3µM standard fluorescein sample; (b) 1.36 nM standard fluorescein sample; (c) 3.2 pM standard fluorescein sample; (d) 1.2 pM FITC labeled arginine; All the samples were prepared using sodium phosphate buffer at pH 11.5.

Fig 1.6 indicates the change of the fluorescence intensity of the preconcentrated plug as a function of time during preconcentration of the sample of 1.36nM standard fluorescein. From the plot, it can be seen that the fluorescence intensity demonstrated almost a linear relationship with the preconcentration time. Combined with the images shown in Fig 1.5, it can be seen that the titanium membrane fabricated within this

manifold performed very powerful ability of preconcentrating dilute samples down to picomolar concentration.
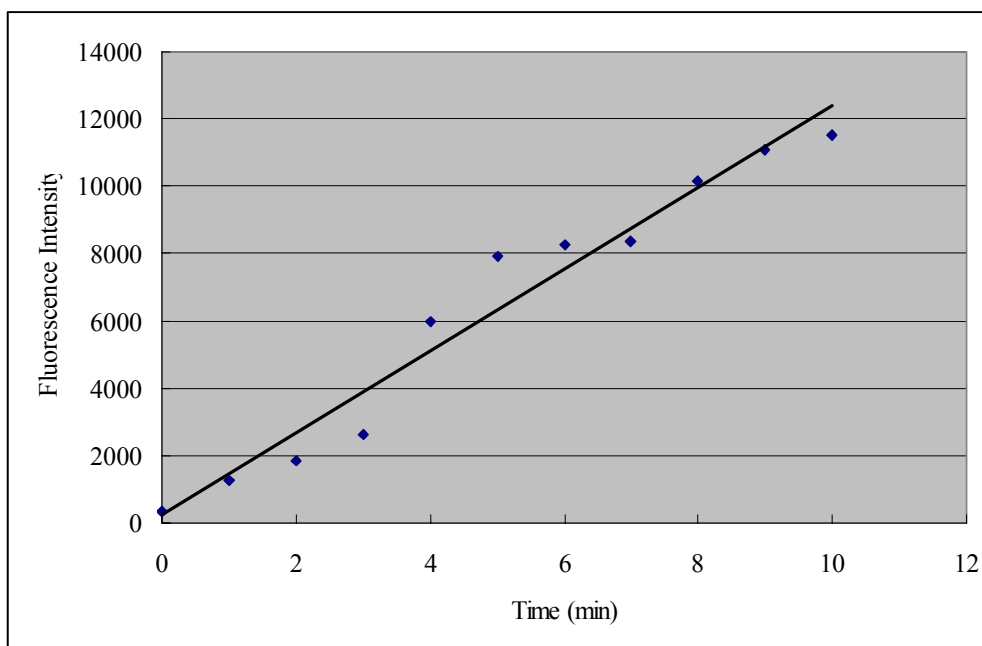
Figure 1.6 Fluorescence intensity vs preconcentration time for 1.36 nM standard fluorescein sample concentrated plug; Sodium phosphate buffer at pH 11.5 was used.

A very interesting phenomenon was found during the preconcentration process. Occasionally the preconcentrated sample plug was located at the right side of the membrane instead of the top side or the left side, as shown in Fig 1.7. The sample concentration used for this case was within the same level as that in Fig 1.5 (c), about 2.7pM standard fluorescein. In addition, comparing these two cases, very much higher intensity was achieved for the second case. Two different membranes fabricated in two glass chips were used for the two cases. For the second case, the position of the membrane was closer to the right corner on the bottom of the intersection, as indicated in Fig 1.8 i.e. n is much less than m. Therefore much more space was left on the top of the membrane, which made it very difficult to form and hold the concentrated sample plug. In contrast, the narrow spacing on the bottom of the membrane was acting an obstacle for concentration. A reasonable explanation might be made using the phenomenon of ion-enrichment and ion-depletion effect associated with nanochannel structures developed and described in the literature (102). In this

phenomenon, both cations and anions were concentrated and depleted on the same side of the nanochannel structures. In this case, it was assumed that the value of n went down to the nanometer scale and thus the negatively charged fluorescein was enriched on one side and depleted on the other side.
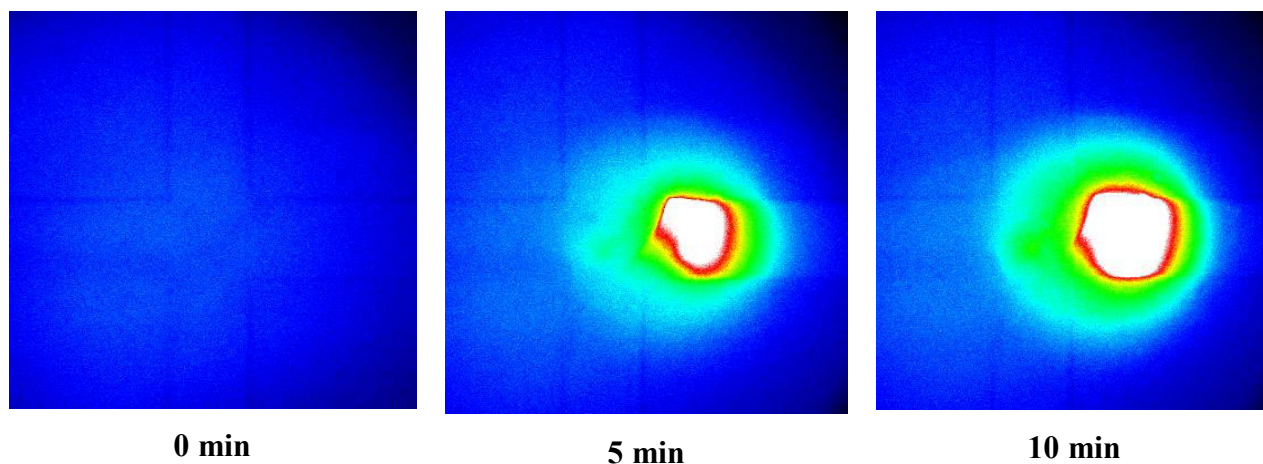

| 0 min | 5 min | 10 min |

Figure 1.7 Images of concentrated plug generated by a membrane on a glass chip for a second case; Sample: 2.7pM standard fluorescein in sodium phosphate buffer at pH 11.5.
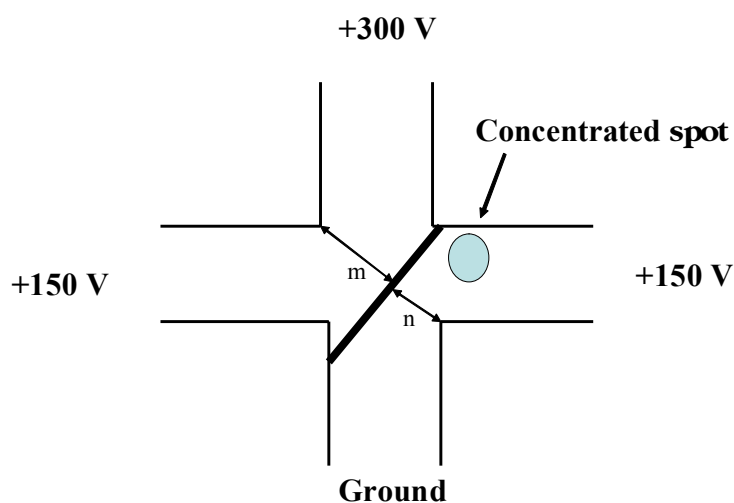
Figure 1.8 Schematic of membrane concentration on a glass chip for a second case

Separation voltage scheme is shown in Fig 1.9. The high voltage in the top reservoir remained as 300 V, while all others were connected to the ground. As a result, under the pumping of the electrokinetic driven, the concentrated plug moved to the right channel as depicted by the block arrow in Fig 1.9. Then it would take a left

turn and get separated and detected. Sometimes the sample plug was too big to pass through the intersection and move to the separation channel. It was struck at the intersection. Therefore the optimized sample plug size and the optimized concentration time should be the aim for the next step of research. Besides, the width and the location of the membrane were critical for acquiring a very good concentration sample plug and afterwards separation performance.

+300 V

Concentrated spot

Ground

Ground

Ground
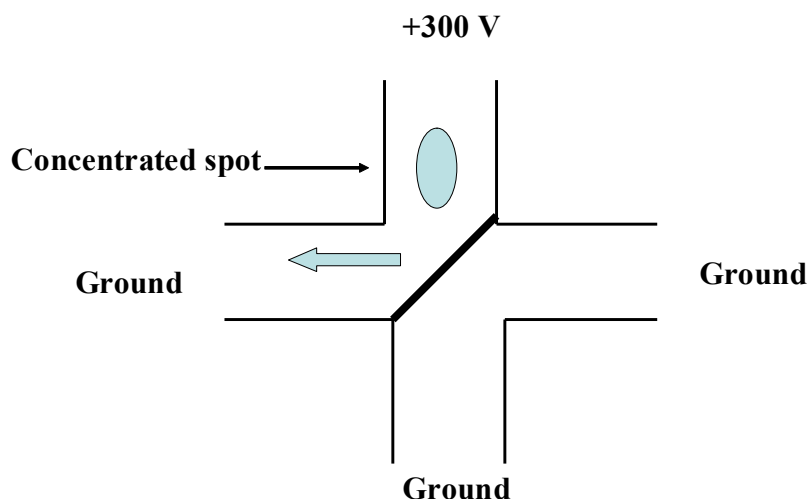
Figure 1.9 Separation voltage scheme for concentrated samples

0.63cm

0.25cm

0.1cm

0.95cm

Detection

3.75cm
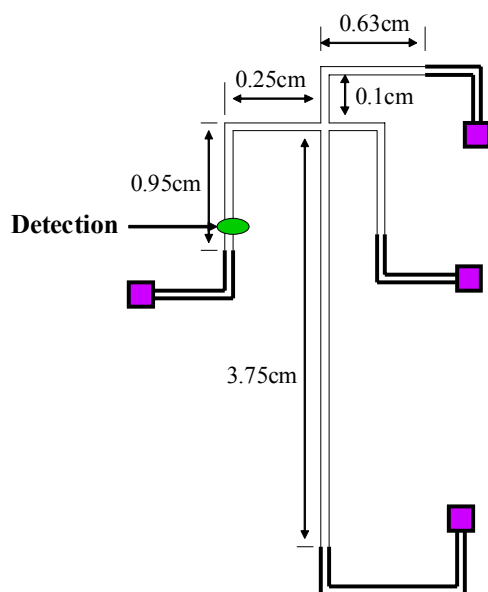
Figure 1.10 Schematic for detection position

Detection was made at the end of the channel connected to the reservoir at the right side, as indicated by the green oval in Fig 1.10. Laser-induced fluorescence was used for detection. The laser was focused at the detection point and was very critical for obtaining a sharp peak with high intensity.

The separation result of a tentative trial made with a fluorescein standard sample using the single point apparatus is given in Fig 1.11. The running conditions for this trial were a sample of 0.3nM fluorescein in the buffer of sodium phosphate at pH 11.5; preconcentration time of 5 min and a separation distance of about 1 cm. In order to obtain very good peaks, further work for optimization of the preconcentration and separation conditions is needed, such as concentration time, separation distance and electric field strength.
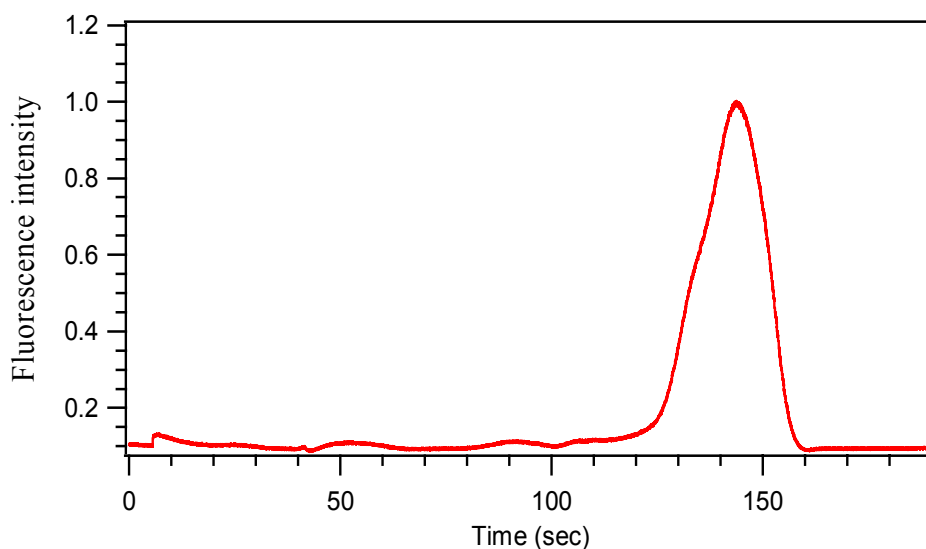
Figure 1.11 Electrophoretic separation of 0.3 nM standard Fluorescein using the voltage scheme indicated in Figure 1.9.

1.4 Conclusions and future work

To sum up, titanium membranes made on glass microchips *in situ* using sol-gel chemistry have the ability to preconcentrate very dilute samples. Future work will focus on the optimization of concentration and separation conditions using standards such as proteins and amino acids in order to obtain very good separation performance, such as preconcentration time, separation distance and separation voltage. Then real samples will be used to check on the availability of this whole system of membrane concentration, separation and detection within the glass microchip.

Chapter 2 Protein Separations by CE using On-column Fluorescence Labeling

Capillary electrophoresis includes a family of related separation techniques conducted in buffer-filled, narrow-bore capillary tubes, usually with an internal diameter (ID) between 25 and 100μm. It is a very efficient separation technique for the analysis of a complex array of both large and small molecules. This technique was originally invented by Arne Tiselius. In 1937, he successfully separated many proteins in a tube by applying an electric field across the tube, which won him the Nobel Prize in chemistry. Since then, capillary electrophoresis has been developed and applied in many fields and demonstrated exceptional separation efficiency. The fundamentals behind CE have been clarified. In 1989, the first fully automated capillary electrophoresis instrument (P/ACE ^{TM} 2000) was introduced by Beckman Instruments.

2.1 Principles of Capillary Electrophoresis (101, 103-105)

2.1.1 Electrophoretic Flow

Capillary electrophoresis is electrophoresis carried out in capillary tubes. The principles that govern electrophoresis are directly applicable to CE. That the differential movement or migration of ions is caused by attraction or repulsion under the influence of an electric field results in the process of electrophoresis. Normally for electrochemistry, when a negative (cathode) and a positive (anode) electrode are immersed in a solution containing charged ions and then a potential difference is applied across the two electrodes, ions of different charges will move towards the electrode of opposite charge, i.e., positive ions (cations) move towards cathode while negative ions (anions) move towards anode. Separations by electrophoresis are operated by the fundamental that ions accelerate in an electric field resulting in

differences in ion velocities. In the process of electrophoresis, a balance between the electric force and the drag or frictional force, also called a steady state, is obtained. The electric force is expressed as

$$F_E = qE$$

Where F_E = electric force

q = ion charge

E = electric field strength

The drag force expression is given by

$$F_F = -fv = -6\pi\eta\, rv$$

Where η = solution viscosity

r = ion radius

f = friction coefficient

The electric force acts in favor of the ion movement while the retarding frictional force slows down the ion motion. The ion almost instantly arrives at a steady state velocity where the electric force equals the frictional force.

$$F_E = -F_F$$

Plug in the first two equations, the ion electrophoretic velocity expression will be resolved as

$$v_{ep} = qE/(6\pi\,\eta\, r)$$

It can be seen clearly that the electrophoretic velocity of an ion is proportional to its charge (q) and the electric field (E) and inversely in proportion to its radius and the solution viscosity (η). Briefly, differences in the charge-to-size ratio of ions are responsible for the differences in migration. An ion with a higher charge and a smaller radius will migrate faster than an ion with a lower charge and larger radius. In addition, the lower the solution viscosity, the higher the flow rate of an ion, and vice versa. The ion charge can be affected by pH changes of the buffer. The ion radius can be affected by the counter-ion present or by any complexing agents used. The qualitative relationship can be defined as the term of electrophoretic mobility (μ_{ep}),

$$\mu_{ep} = q/(6\pi\,\eta\, r)$$

Thus, electrophoretic velocity can also be expressed as,

$$v_{ep} = \mu_{ep} E$$

Electrophoretic mobility is a constant for a given ion and a given constant buffer system. It indicates how fast a given ion may migrate through a given buffer and determines migration velocity of an ion. The differences in electrophoretic mobility are the basis for the separation of ion mixtures.

2.1.2 Electroosmotic Flow (EOF)

Electroosmosis refers to the movement of the bulk buffer solution in a capillary tube under an electric field. For capillary electrophoresis, since an electric field is applied through a narrow-bore fused-silica capillary tube used under most conditions, a different form of ion movement occurs. Under aqueous conditions, the ionizable silanol groups on the internal surface are easily ionized, leading to a negatively charged surface along the capillary wall as indicated by the following equation.

$$S_iOH \rightarrow S_iO^- + H^+ \quad (\text{pH} > 2)$$
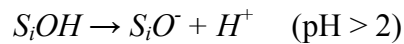
This negatively charged surface is counterbalanced by positive ions in the buffer, giving rise to an electric double layer and a potential difference (zeta potential) close to the wall. As shown in Fig 2.1 by Stern's model, the innermost layer of positive ions is tightly bound to the surface and cannot move. It is also called the compact layer or Helholtz or Stern layer, which can only neutralize the negative charge. The second layer contains solvated, mobile positive ions which may diffuse by thermal motion and neutralize the remaining negative charges. This charge double layer creates a potential difference which is called zeta potential. The zeta potential is the potential difference across the different part of the double layer and decreases exponentially with increasing distance from the capillary wall surface. The zeta potential is determined by surface charge density. For negatively charged silica capillary surface, the surface charge density increases with increase in pH of the buffer and decreases with increase in the ionic strength of the buffer, that is, the concentration of the buffer. Under the influence of an electric field, the positive ions in the diffuse layer migrate towards the cathode. Their movement will carry the bulk

buffer with them and lead to the bulk buffer flow towards the cathode too, which is called electroosmotic flow. This pumping action is called electroosmosis. The electroosmotic flow rate is expressed by

$$v_{eo} = \varepsilon\,\zeta\,E/(4\pi\eta)$$

Where ε = dielectric constant of the buffer solution

ζ = zeta potential at the capillary and buffer interface

The equations of EOF are similar to those of electrophoresis. The electroosmotic mobility can be described as

$$\mu_{eo} = \varepsilon\,\zeta\,/(4\pi\eta)$$

As the electrophoretic velocity does, the electroosmotic flow rate can also be expressed as

$$v_{eo} = \mu_{eo}\,E$$

It can be seen that electroosmotic mobility is mainly affected by the dielectric constant of the buffer solution, zeta potential and the buffer viscosity. It is proportional to the dielectric constant, the zeta potential and inversely proportional to the viscosity of the buffer. The zeta potential depends on the electrostatic nature of the capillary surface, which is pH dependent, and the ionic strength of the buffer. At low pH, EOF mobility is reduced because the charged SiO^- is converted to neutral $SiOH$ by protons. It also decreases as ionic strength of the buffer increases because increase in ionic strength can result in the compression of the double layer and thus the decrease in zeta potential. EOF also can be reduced by using a material that is able to suppress ionization of the silanol groups to modify the capillary wall surface. Polyacrylamide and methylcellulose are examples of such materials.
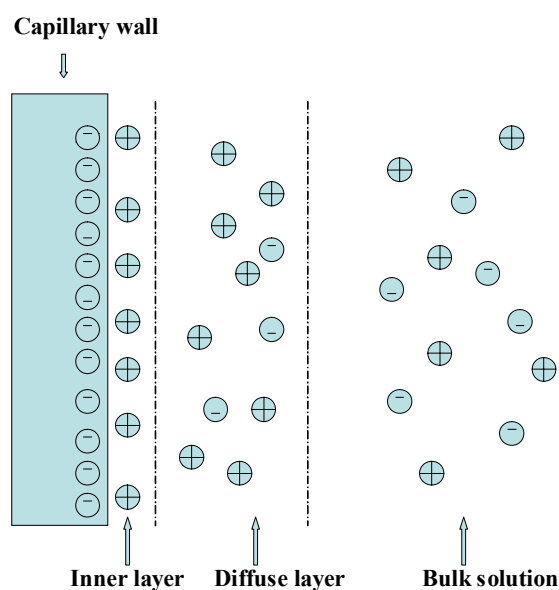
Figure 2.1 Representation of the double layer charge distribution at the capillary wall (Stern's model)

2.1.3 Apparent Flow

The apparent migration velocity , v_{app}, also can be called as electrokinetic velocity , v_{ek} , of an ion is a vector sum of the electrophoretic velocity, v_{ep}, and the electroosmotic flow velocity, v_{eo}, of the buffer.

$$v_{app} = v_{ep} + v_{eo}$$
$$= \mu_{ep} E + \mu_{eo} E$$
$$= (\mu_{ep} + \mu_{eo}) E$$

The apparent mobility, μ_{app}, of the ion equals the vector sum of the electrophoretic mobility, μ_{ep}, of the ion and the electroosmotic mobility, μ_{eo}, of the buffer.

$$\mu_{app} = \mu_{ep} + \mu_{eo}$$

The apparent migration velocity can be rewritten as,

$$v_{app} = \mu_{app} E$$

One unique feature of EOF is that it leads to all the species- cations, anions and neutrals moving in the same direction, from anode to cathode for negative

charged fused -silica surfaces. Electrophoretic flow of a cation is in the same direction as the electroosmotic flow, and thus μ_{ep} and μ_{eo} are additive and the apparent mobility (μ_{app}) is higher than μ_{ep}. On the other hand, the electrophoretic flow of an anion is against the direction of EOF. However, the net migration of an anion is also towards to the cathode, since EOF is generally higher than the electrophoretic flow of an anion when pH > 3. Cations and anions are separated based on the differences in their apparent mobility. Neutral solutes are all carried in the same direction at the velocity of EOF and they are not able to get separated. Therefore, cations move the fastest; followed by neutrals and anions are the slowest.

A benefit of EOF in CE is the flat flow profile. Since the driving force (i.e., charge on the capillary wall) is uniformly distributed along the capillary, there is no pressure drop within the capillary and the flow is nearly uniform across the capillary. That is, the velocities at all points along the radius are the same. It is beneficial because it doesn't directly contribute to the dispersion of the solute zone and minimizes zone band broadening, which results in high separation efficiencies that allow separations on the basis of mobility differences as small as 0.05%, as compared with pressure-driven flow which gives a parabolic flow profile that causes band broadening. The profile differences are illustrated in Figure 2.2.
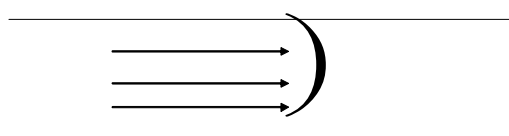
(a) Laminar flow
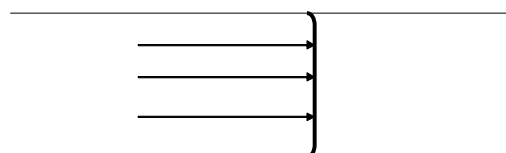
(b) Electroosmotic flow

Figure 2.2 Flow profiles

Many methods have been reported to modify the internal surface of the fused silica capillary to suppress EOF and reduce adsorption of solutes, such as covalent attachment of silanes with neutral or hydrophilic components. The direction of EOF can be reversed from cathode to anode by adding a positively charged surfactant like cetyltrimethylammonium bromide (CTAB) to the buffer, since the surfactants form a bilayer bound tightly to the negatively charged capillary wall and change the charge of the wall from negative to positive.

2.1.4 Factors Affecting Separation

The van Deemter equation models separation efficiency of some separation techniques such as chromatography including CE and field-flow fractionation.

$$H = A + B/\upsilon + C\upsilon$$

This equation relates the plate height (H) to the velocity (υ) of the carrier gas or liquid along the separation axis. The lower is the value of H; the higher is the separation efficiency. The terms of A, B and C are constants. The A term is the effect of parabolic flow and multiple paths. It goes zero in CE due to the flat flow profile resulted from EOF. The C term refers to mass transfer term and it also goes zero in CE since no stationary phase exists and the separation is performed in a single liquid phase. That is, two of the three contributing plate height terms in this equation are eliminated. As a result, the longitudinal diffusion (B term) is the only source of band broadening under ideal conditions. Under typical conditions, 50,000 to 500,000 theoretical plates count can be achieved by CE, which is an order-of-magnitude higher than HPLC separation.

Band broadening refers to the process of dilution of analyte concentration as a result that the different regions of the anayte migrate at different velocity. Diffusion is the main source of band broadening. There are a number of other sources that might contribute to band broadening and thus reduce separation performance. The sources include sample injection volume, detection window length, adsorption, electrodispersion, joule heating and so on (101).

A large sample injection volume can cause solute band broadening, especially for fast separations in short capillary. The injection plug length should be controlled less than 5% of the separation distance (i.e., the distance from the injection point to the detection point).

Temperature variation due to joule heating produced by the resistance of the bulk buffer to the flow of the electrical current in the capillary might affect the solute band. The heat generated (H) equals the product of the applied voltage (V) and the electric current (I) and the migration time (t).

$$H = VIt$$

The large surface to volume ratio of the capillary allows for the efficient heat dissipation and application of high electric field. However if the heat dissipation is not sufficient, especially under high electric field strength and some heat remains creating a temperature gradient along the capillary radius. The temperature in the center along the capillary radius is higher than that close to the capillary wall, leading to non-uniformity of the buffer viscosity. The buffer in the center is less viscous than that close to the capillary wall, resulting in a parabolic flow profile due to the non-uniformity of analyte migration.

Electrodispersion is caused because of the fact that the conductivity of the running buffer does not match that of the sample plug.

Long detection window is used to enhance the detection sensitivity, but it can reduce the separation efficiency. Other factors such as analyte adsorption to the capillary wall, laminar flow caused by the unequal buffer reservoir heights also contribute to band broadening and thus degrade separation efficiency.

These factors including molecular diffusion are additive for peak width. Peak width equals 4 times of the standard deviation of the peak (σ).

$$w = 4\sigma$$

The Einstein-Smoluchowski equation gives the σ expression caused by molecular diffusion alone, which a Gaussian shaped analyte band is assumed.

$$\sigma^2_{diffusion} = 2Dt$$

The total standard deviation of the peak width can be described as

$$\sigma^2_{total} = \sigma^2_{diffusion} + \sigma^2_{injection} + \sigma^2_{heating}$$
$$+ \sigma^2_{electrodispersion} + \sigma^2_{detection\ window} + \sigma^2_{adsorption}$$

In addition to plate height (H), peak width (w), other analytical parameters for indicating CE separation efficiency contains theoretical plate count (N) and resolution between two components (R). The relationship among these parameters can be expressed as the following formula. Resolution is formulated by the difference in baseline widths (w) and migration times of the two peaks.

$$N = l_{det}/H$$
$$= l^2_{det}/\sigma^2_{total}$$
$$R = (t_2 - t_1)/4\sigma$$
$$= 2(t_2 - t_1)/(w_1 + w_2)$$

Theoretical plate counts indicates band broadening quantitatively. A high value means the solute zone length is relatively short over a long separation distance, indicating good separation performance, while a low number shows a poor separation.

For diffusion limited band broadening under ideal conditions, σ equals 2Dt. D is diffusion coefficient of the solute. T is migration time. L is capillary length, V is applied voltage.

$$\sigma = 2Dt;$$
$$t = l_{det}/v_{app};$$
$$v_{app} = \mu_{app}\ E;$$
$$E = L/V$$

From these formulas, the theoretical plate counts can be rewritten in terms of the apparent mobility,

$$N = \mu_{app}\ El_{det}/(2D)$$

Resolution between two components can be described as

$$R_s = 0.25(\mu_{app1} - \mu_{app2})\ \{V/[2D(\bar{u}_{ep} + \mu_{eo})]\}^{1/2}$$

It can be seen that a high theoretical plate count can be obtained by increasing mobility, electric field strength and detection distance. A large difference in mobility of the two components can help achieve good resolution.

2.2 Instrument of CE

CE system is very simple. Capillary tube and an electric field are needed for CE operation. Capillary tube is the key part of CE system. Fused silica is commonly used to produce capillary tube because of its intrinsic properties such as transparency and high thermal conductance. The internal diameter of the capillary tube is normally between 25-100μm. A high voltage power supply, normally between 0-30kV, is needed. A diagram of CE system is indicated in Fig 2.3.
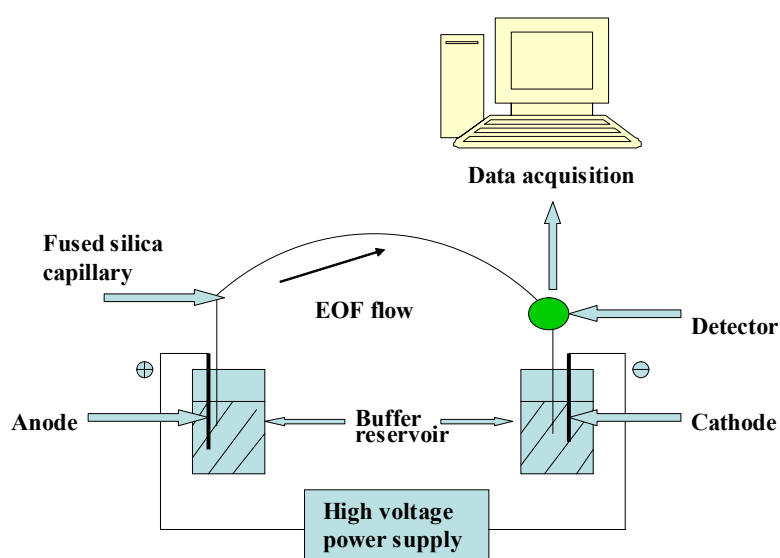
Figure 2.3 Schematic diagram of CE system

In the CE operation, the two ends of the capillary are connected to electrodes through two separate buffer containers. The two electrodes are connected to the high voltage supply. The capillary is first filled with the buffer. Then the analyte is introduced into the capillary by replacing one of the buffer containers with the sample reservoir. Normally the injection is made on the anode end. After the buffer container is put back, a voltage is applied across the capillary and separation is carried out. Usually detection, either on-column or off-column detection, is made near the cathode end. Software packages are used to control the CE instrument.

45

2.3 Sample Injection

CE has the capability to inject extremely small volumes of a sample. Normally the injection volumes fall in the range from picoliters to nanoliters. Either electrokinetic or hydrodynamic injection can be employed. Electrokinetic injection is conducted by simply applying a voltage for a certain time, usually within the range of seconds. Many factors affect electrokinetic injection, such as injection time, voltage and the property of the capillary wall. The following expression describes the relation between the moles of each injected analyte (Q_i) and the apparent velocity of each analyte (v_{app}), the injection time (t), the ratio of conductivities of the buffer and the sample (k_b/k_s). In the expression, r is the capillary radius and C_i is the molar concentration of each analyte.

$$Q_i = v_{app} \, (k_b/k_s) t \pi r^2 C_i$$

A problem associated with electrokinetic injection is the analyte dispersion caused by the differences in mobility of different analytes. As a result, the concentrations in the injected sample plug are different from those in the original sample.

A pressure difference between the two ends of the capillary is applied to achieve hydrodynamic injection. A pressure difference can be made by applying vacuum. Siphoning also can be used to generate a pressure difference, simply by raising the sample reservoir a certain height higher than the buffer reservoir on the other end. The Poiseuille equation gives the volume of the injected sample.

$$V_c = \Delta P \pi d^4 t / 128 \eta L$$

Where V_c = the calculated injection volume

ΔP = pressure difference

d = inner diameter of the capillary

t = injection time

η = sample viscosity

L = capillary length

The sample injected by hydrodynamic injection is the same as the original sample. However, in regard to precision and accuracy, electrokinetic injection is more precise and accurate than hydrodynamic injection (106).The latter is less reproducible. In addition, electrokinetic injection is easy to handle and the velocity discrimination of the analytes during injection might contribute to selectivity (106).

2.4 Separation Modes of CE

CE can be divided into several separation techniques. The main examples include capillary zone electrophoresis (CZE), capillary gel electrophoresis (CGE), capillary isoelectric focusing (CIEF), micellar electrokinetic capillary chromatography (MEKC), capillary isotachophoresis et al.

Capillary zone electrophoresis (CZE) is also named as free-solution CE (FSCE). It is the simplest mode of CE family. Homogeneity of the running buffer and constant field strength through the whole capillary are the fundamental of this mode. The separation mainly depends on the pH modified dissociation of acidic groups or the protonation of basic groups of analytes. A narrow zone of a sample is introduced into the capillary, surrounded by the running buffer. As a voltage is applied across the capillary, each analyte in the sample zone moves at a velocity based on its apparent mobility. Under ideal conditions, each analyte will form an individual zone and get separated from each other. All the neutrals will stay in one zone and separate from the charged analytes, but they cannot separate from each other because they move at the same flow rate as EOF.

Capillary gel electrophoresis (CGE) is adapted from the traditional slab gel electrophoresis. It is carried out in a polymeric gel medium. The polymer network serves as a sieve in which smaller molecules move quicker than large molecules by decreasing the analyte diffusion velocity and the adsorption of the analyte to the capillary wall. Since EOF is suppressed, short capillaries can be used, thus reducing analysis time and increasing efficiency. Molecules are separated based on the differences in their size in a nonconvective medium. CGE is very suitable for the

separation of large molecules like proteins and DNAs. Non-crosslinked polymer, such as cellulose derivatives and polyacrylamide, and crosslinked gels, such as polyacryamide and agarose can be used as gel media. Non-crosslinked polymers can be easily removed out of the capillary and easily refilled to form a fresh capillary. By modifying the concentration of the monomer and the degree of cross-linking for crosslinked polymers, the resolution can be easily optimized.

Capillary isoelectric focusing (CIEF) is a separation form of CE on the basis of differences in the isoelectric point (pI) of sample analytes. In this technique, a charged analyte is driven through a pH gradient until it encounters a pH at which it has a zero net charge and stops migration. Thus the analyte is focused into a tight zone, which is then driven through the detector by pressure or chemical methods. If the analyte molecules in the focused zone diffuse away from the zone, they will immediately gain or lose protons and therefore obtain charges. The charged molecules will be forced back to the zone center of the zero net charge point. A steady state in which the zones are stationary and sharply focused will be reached in the end. The expression of the variance of Gaussian distribution describes the width of the focused zone.

$$\sigma^2 = (D/E) \ (d(pH)/d\mu_{app}) \ (dx/pH)$$

To obtain a sharper zone, i.e., a smaller variance, a low diffusion coefficient (D) and high field strength (E) is preferred. A high rate of change of mobility with pH ($d\mu_{app} / d(pH)$) and a high slope of the pH gradient ($d(pH)/dx$) are favorable. A difference between the two *pI*s required for a complete separation of two analytes must be higher than 4σ.

A pH gradient is created using a series of zwitterions (ampholytes) under an electric field. They are mixtures of 600-700 different zwitterionic compounds exhibiting a series of pIs between 3 and 10. Positively charged ampholytes move towards the cathode, while negative charged move to the anode, leading to an increase of pH in the end of cathode and a decrease of pH at the anode end. When ampholytes arrives at their own pI with a zero net charge, they discontinue migrating, generating a

stable pH gradient. A narrower pH range can be obtained using a large number of ampholytes.

CIEF allows amphoteric molecules to be separated such as peptides, amino acids and proteins. Free solutions or polymer gels can be used as the separation medium. EOF and other convective forces should be eliminated or highly suppressed in order to achieve effective CIEF. However, on the condition that the electrophoretic velocity is greater than EOF, CIEF still can be conducted. One thing to pay attention to is the pH of buffer electrolytes. In the cathode end, a buffer with a higher pH than the pIs of all the basic ampholytes should be used, while a buffer with a lower value of pH than the pIs of all the acidic amphoytes should be used in the anode end. Doing this is to keeping buffers from migrating into the capillary from the buffer reservoirs.

Micellar electrokinetic capillary chromatography (MECC) can not only be applied to separate charged compounds, but also neutrals. Micelles formed by adding a micelle forming reagent to the separation buffer are used to serve as a pseudo-stationary phase to separate neutrals. A micelle forming reagent is an amphiphilic monomer (also called surfactant) which has a hydrophilic head and a hydrophobic tail. The hydrophilic head can be cationic, anionic, nonionic or zwitterionic, while the hydrophobic tail can be a straight or branched chain of hydrocarbon. Sodium dodecyl sulfate is the most commonly used micelle forming reagent. When the concentration of the micelle forming reagent is higher than its critical micelle concentration, the molecules of the micelle forming reagent are aggregated together because of the polarity of the buffer. In aqueous buffer, spherical micelles take the form of the hydrophobic tails facing inside and the hydrophilic heads outside.

The separation principle in MECC is achieved by the combined result of the differential partitioning of molecules between the buffer and the micelles and differential migrations of ionic molecules. Analytes and micelles can interact with each other through a number of types of forces such as hydrophobic, electrostatic and H-bonding interactions. The neutral molecules migrate at the rate of EOF before the micelles are added. The micelles move at a velocity lower than the EOF. When the neutral is trapped by a micelle, it moves at the same velocity as the micelle. The

49

separation of analytes between the buffer and micelles can be adjusted by modifying the concentration or the type of a surfactant. It also can be controlled by adding some additives to the buffer such as ionic salts, chiral selectors; ion-pairing et al. Variation in temperature and pH also affects separation. MEKC is very valuable in separating mixtures of charged and neutral analytes.

Capillary isotachophoresis (CITP) is a separation technique using a moving boundary electrophoretic mode. Two buffer solutions are used to generate a steady state in which all analytes zones migrate at the same rate. The sample is added between the leading buffer with a higher mobility and the trailing buffer with a lower mobility compared with the mobility of the analytes. Differences in the velocities of analytes in the sample zone are the basis for separation. After separation, each analyte remains in different bands and move at the same rate, resulting in a steady state of stacking. CITP cannot be utilized to separate both cations and anions in a single run.

Other modes of CE have been developed and applied, such as electrokinetic chromatography (EKC), micro emulsion electrokinetic chromatography (MEEKC) and capillary electrochromatography (CEC). Many combinations of different modes of separation have been made for multidimensional separations, such as LC-CE, CITP-CZE, IEC-CZE (IEC stands for ion-exchange chromatography) (107). Even combinations of three separation techniques are available for 3-D separation system. For example, Janini and coworkers have reported a powerful system of coupling IEF, RP-HPLC and cation exchange chromatography which possesses the ability of analyzing very complex mixtures (108). In two or multidimensional separation, IEP and CITP modes are frequently utilized as the first step of preconcentration or/and preseparation.

2.5 Methods of Detection for CE

Many detection methods have been combined with CE. Some commonly used detection methods and their limit of detection (LOD) are listed in the table 1.1 of last chapter.

UV-absorption detection is the universal method for monitoring CE separations due to the strong absorption of a UV radiation (200-220nm). Laser-induced fluorescence (LIF) possesses the highest sensitivity and has the potential to detect even a single molecule. But LIF requires the derivatization of analytes, which might result in multiple labeling and thus affect detection precision. The ideal detection technique is mass spectroscopy which provides advantages of high sensitivity and selectivity. It enables both analytical and structural determination. The coupling of CE with MS has been growing. But the instrument of MS is very expensive and the analysis costs much in terms of analysis time, sample consumption.

2.6 Applications of CE

CE has been highly accepted as an efficient separation technique for qualitative determination. It offers advantages of simplicity, high resolution separation, and minimal cost. CE operation is very rapid and takes little time. It consumes little sample and reagents. Comparison of migration times with those of standards is the best and simplest method to determine CE peaks qualitatively. Additional information is needed for further confirmation. For example, Spectrophotometric detection can be used to compare the ratio of absorbance at a series of wavelengths in the unknown with the ratio in the suspected compound, therefore giving further information for peak identity. In addition, amperometric detection also can be employed to obtain the ratio of currents from two different electrical potentials for further confirmation.

CE has not been fully established as a method of quantitative analysis. However, it offers useful information about the concentration of an analyte in a sample. Quantitative analysis can be achieved by comparing the analyte's peak area or height with those of calibration standards because peak height directly relates to the concentration of the analyte and peak width directly relates to the residence time in the detector. Internal standardization techniques using internal calibration have been developed for quantitative analysis (109-111). It is aimed to reduce the sample bias

caused by electrokinetic injection and provides better precision. Normally, a known concentration of an internal standard is added to the sample. The mixture is performed by CE analysis; therefore the ratio of peak area or height of the analyte to that of the internal standard can be obtained. A calibration curve should be prepared by plotting ratios of peak area or height of the calibration standard to that of the internal standard against the concentrations of the calibration standard.

A large number of papers about applications of CE have been published (107, 112-114). CE analysis has been applied in many fields such as biological and pharmaceutical areas and has demonstrated tremendous potentials for a wide range of compounds from small molecules, such as inorganic ions, organic acids, peptides, drugs and nucleosides, to large compounds like proteins, hormones, nucleic acids. Its application has even been extended to single cell analysis. Kvasnicka reviewed applications of CE in food authentication which is used to check whether the commercial food matches its description (112). A review on the recent advancement of pharmacokinetic study using CE has been published by Sung (113). Kraly and coworkers summarized bioanalytical applications of CE including single cell analysis, neuroscience, DNA analysis, carbohydrates and lipids analysis (114). The detailed applications of CE (including CEC) of peptides have been presented in the reference 106. The covered areas in this review contain quality control and determination of purity, determination in biomatrices, monitoring of chemical and enzymatical reactions and physical changes and amino acid sequence analysis et al.

2.7 Derivatization of Samples

As mentioned above, LIF is the most sensitive detection method and very suitable for detection of very dilute samples. It is commonly combined with CE as a detector. The fundamentals of fluorescence detection have been covered in the first chapter. However, most biologically important compounds are not natively fluorescent. The compounds that are natively fluorescent usually need high energy excitation in the region of UV wavelengths such as the spectral region of 260-300nm

for aromatic amino acids or proteins containing aromatic amino acids. UV lasers in this spectral region are very expensive and unreliable. Those limitations make it very important to modify and label nonfluorescent compounds with a fluorescent labeling reagent by chemical reactions to generate fluorescence in LIF (115). Fluorogenic stains are another type of fluorescence labeling reagents. They are naturally nonfluorescent reagents, but they can generate a fluorescent product when they react with their target such as primary amines (116).

There are problems associated with fluorescence labeling reactions (116). Under aqueous conditions, most fluorescent labeling reagents experience hydrolysis. For an efficient labeling, the hydrolysis reactions make it necessary to use labeling reagents with high concentrations. However, the use of high concentration of labeling reagents and hydrolysis products lead to high background signal, suppressing the fluorescence signal of analytes, especially very dilute samples. In addition, multiple labeling is an intrinsic problem. Normally an analyte such as a protein possess many labeling sites (primary amines for proteins). The labeling reactions don't go to completion, resulting in many different labeling products with different mobility, therefore very complex broad peak profiles. To collapse multiple labeling, a reagent (often a surfactant such as sodium dodecyl sulfate (SDS)) can be added to the sample to form neutral reaction products along with an ion pair reagent to neutralize unreacted labeling sites (117). The interaction between SDS and a protein occurs through the hydrophobic attraction between the long alkane chain of SDS and the hydrophobic regions of the protein, and the ionic interaction between the anionic sulfate group of SDS and the positively charged side chains of unlabeled residues (118). On the other hand, fuorogenic reagents can reduce the background by orders of magnitude compared with fluorescent reagents. Therefore they are more suitable for labeling very dilute samples.

Three labeling methods can be made for CE—precolumn, on-column and postcolumn labeling. Precolumn labeling is the most common, but it consumes relatively a large amount of analytes and labeling reagents. A postcolumn labeling reaction goes slowly, thus limiting the detection. In contrast, on-column labeling is

more suitable for dilute samples since sample evaporation and sample dilution and sample loss to the capillary wall can be minimized (115).

A labeling reagent for labeling a compound should have an excitation wavelength that matches one of the listed lines of a commonly used laser. In this work, a fluorogenic stain-3-(2-furoyl) quinoline-2-carboxaldehyde (FQ) which matches the 488nm line of argon ion laser was used and on-column labeling format was employed. When a nucleophile such as cyanide ion is present, FQ will react with an amino acid to generate an intensely fluorescent isoindole whose absorption maximum closely matches the 488nm radiation of the argon-ion laser (118).
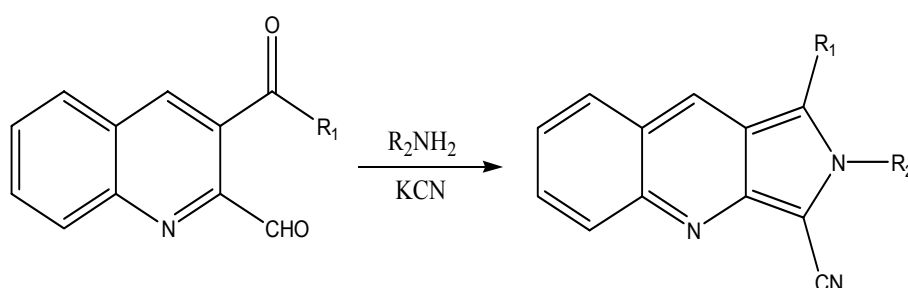
2.8 Experimental Section

2.8.1 Reagents

3-(2-furoyl) quinoline-2-carboxaldehyde (FQ) in a unit size of 10mg was obtained from Molecular Probes (Eugene, OR). Lysozyme, methanol and dimethylsulfoxide (DMSO) were purchased from Fisher (Pittsburg, PA). Myoglobin was obtained from Sigma (St. Louis, MO). The proteins were used as received. A 10mM stock solution of FQ was prepared by dissolving the 10mg of FQ in 4.0mL methanol. 20μL aliquots were transferred to 1000mL eppendorf vials and methanol was removed under vacuum using a dessicator. The dried FQ aliquots were kept at -20℃ in the freezer until they were ready for use. The drying step was necessary since FQ degrades in solution even if kept at -20℃. Sodium dodecyl sulfate (SDS) was obtained from Sigma (St. Louis, MO), Sodium tetraborate (Borax) was purchased from Fisher (Pittsburg, PA). Potassium cyanide (KCN) was obtained from Mallinckrodt (St. Louis, MO). The running buffer of 2.5mM borax and 5mM SDS

with a pH of 9.5 was prepared for CZE analysis. A stock solution of KCN was made in the running buffer at a concentration of 200mM. A 20mM solution of KCN was prepared by 1:10 dilution using the stock solution. A stock solution of 0.8 mM lysozyme and 1.0mM myoglobin was made using the running buffer. Then the stock solution was diluted 1000-fold to get the μM solution using the running buffer. All solutions were made with distilled, deionized water from a Barnstead Nanopure System (Dubuque, IA) and then filtered by 0.45μm Acrodiscs (Gelman Sciences, Ann Arbor, MI).

2.8.2 Instruments

Experiments were performed using an in-house built CE instrument with a LIF detector. The LIF detector was described in detailed in the last chapter. The 488nm beam of an argon ion laser was used as excitation.

2.8.3 Precolumn Labeling and CE Running Procedure

18μL of a sample solution and 2μL of the 20mM KCN solution were added to a vial containing the dried FQ from 20μL aliquot and vortexed for 5s. The labeling reaction was allowed from 10s to 1h.

Separations were carried out in a bare capillary by applying electric fields. The polyimide coating was removed for detection by a gentle flame. Solutions were injected by electrokinetic injection. The buffer of 2.5mM borax and 5mM SDS at pH 9.5 was used as the running fluid.

2.8.4 On-column Labeling and CE Running Procedure

The labeling reaction was performed in the capillary. The FQ solution was prepared by adding 20μL of the running buffer to a vial of dried FQ. The protein/KCN solution was made by adding 18μL of the protein solution and 2μL of the 20mM KCN solution. Solutions were introduced hydrodynamically by a vertical displacement of 10cm for 20s. The protein and KCN solution was injected first and then followed by the FQ solution. In between, the capillary tip was rinsed by dipping into a vial

containing the running buffer to minimize the contamination of the FQ solution. Another vial containing the buffer heated to around 65℃ was used to hold the capillary tip to improve efficiency of the labeling reaction. The labeling reaction was allowed to react around 30s. Then a voltage was applied for separation. The buffer of 2.5mM borax and 5mM SDS at pH 9.5 was used as the running fluid.

Potassium cyanide (KCN) is very poisonous and generates lethal HCN gas when encountering acids. A basic buffer should be used to prepare the stock solution of KCN. Wastes containing KCN should be neutralized by a strong base solution such as sodium hydroxide (NaOH) or Potassium hydroxide (KOH).

2.9 Results and Discussion

As discussed in the first section, theoretical plate number and resolution can be expressed by the following two equations individually.

$$N = \mu_{app} E l_{det}/2D$$

$$R_s = 0.25(\mu_{app1} - \mu_{app2})\{V/2D(\bar{u}_{ep} + \mu_{eo})\}^{1/2}$$

It is clear that high separation efficiency can be achieved by increasing electric field strength (E) and/or detection distance (l_{det}). Enhancing voltage may give a good resolution. However, those variables cannot be raised without limitation. For example, a longer detection distance leads to longer separation time, therefore wider peaks ($\sigma = 2Dt$). The resultant band broadening might cause poor resolution. In addition, an applied high voltage may result in joule heating which contributes to band broadening.

This work was aimed to find out the optimal running conditions for separation using the home-made CE-LIF. FQ, a fluorogenic labeling reagent, was employed to reduce fluorescent background. Techniques of precolumn and on-column labeling were compared.

For the on-column labeling of FQ, at pH of 9.5, FQ is neutral while most proteins are negatively charged. The apparent mobility of FQ is higher than those of proteins. FQ moves faster than proteins. Thus FQ is introduced to the capillary first

and then followed by protein samples. They meet and react in the capillary to form fluorescent products for detection.

2.9.1 Comparison of Labeling Methods

The following consistent conditions were used to compare precolumn and on-column labeling. The sample used was a mixture of 1.6 µM lysozyme and 2.0µM myoglobin in the buffer of 2.5mM borax and 5mM SDS with a pH of 9.5. A capillary length of 42cm with a detection distance of 28cm was employed. The electric field strength applied was 400V/cm. Electrokinetic injection was made for 5s for precolumn labeling while hydrodynamic injection was utilized for on-column injection with a vertical displacement of 10cm for 20s.
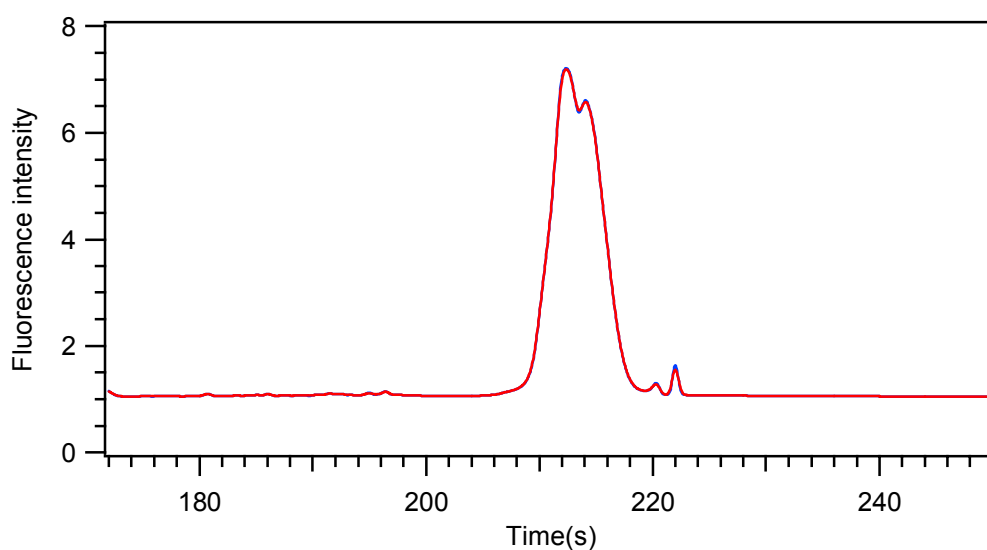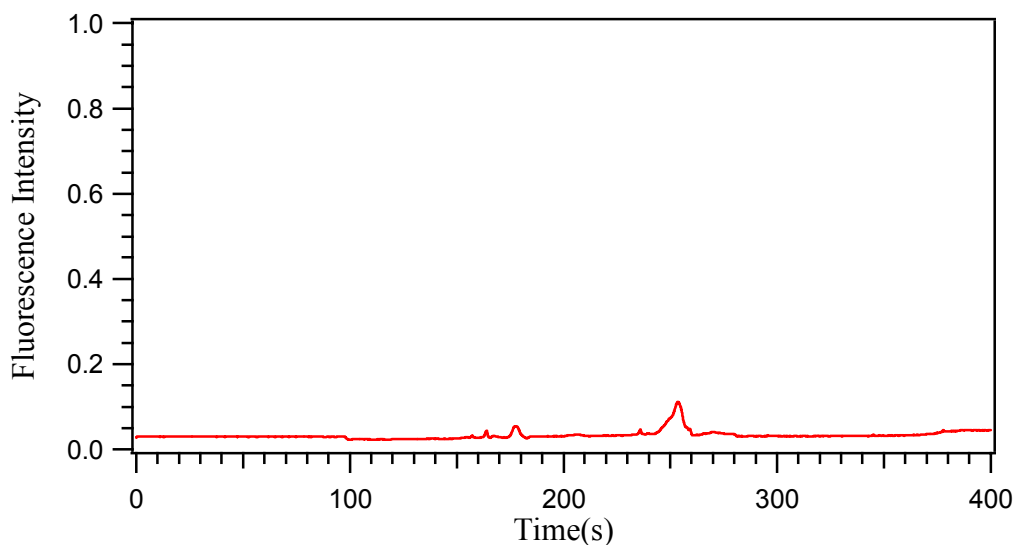

Figure2. 4 Electropherogram for 1.6 µM lysozyme and 2.0µM myoglobin;

FQ precolumn labeling; Electric field strength of 400 V/cm;

The buffer of 2.5mM borax and 5mM SDS with a pH of 9.5;

Detection distance of 28cm
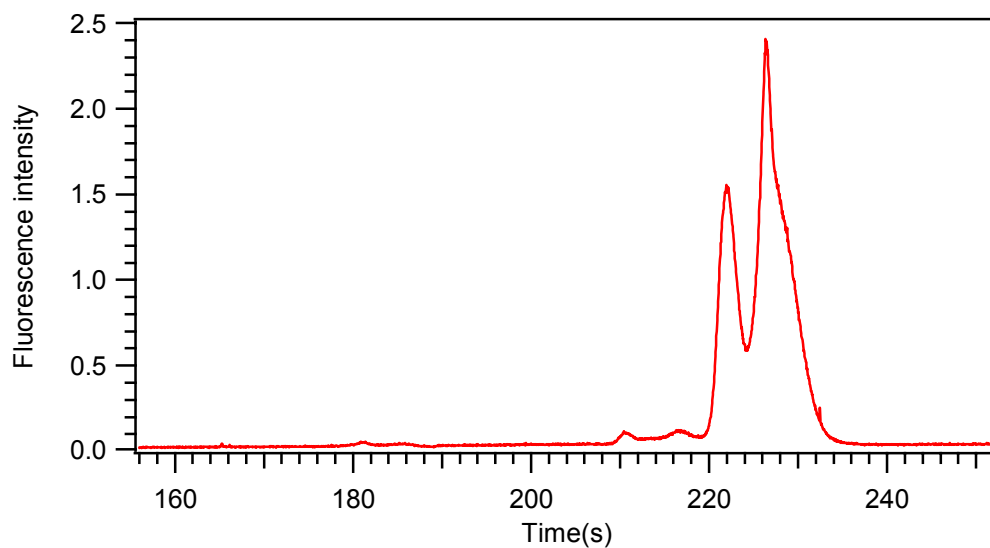
Figure 2.5 Electropherogram for 1.6 µM lysozyme and 2.0µM myoglobin;

FQ on-column labeling; Electric field strength of 400 V/cm;

The buffer of 2.5mM borax and 5mM SDS with a pH of 9.5;

Detection distance of 28cm

It can be seen clearly that the two proteins were not resolved using precolumn labeling under this condition, while much better resolution was obtained for on-column labeling. Therefore for all the following runs, on-column labeling was taken.

Fig 2.6 gives the electropherogram for the blank (the solution of FQ with KCN in water). The same running conditions and the exact running procedure as those of Fig 2.5 were used.

Figure 2.6 Electropherogram for the blank of a solution of FQ and KCN in water

FQ on-column labeling; Electric field strength of 400 V/cm;

The buffer of 2.5mM borax and 5mM SDS with a pH of 9.5;

Detection distance of 28 cm

2.9.2 Comparison of Different Solvents for FQ

The solubility of FQ in water is limited. For 10mM FQ solution in water used, some precipitates might be formed, which might have some negative influence on separation performance. 5mM FQ solution was tried for on-column labeling scheme. But probably because of the short on-column labeling reaction time and the difficulty of mixing of FQ with samples on column, no good signal was obtained. In order to increase the solubility of FQ without decreasing its concentration, DMSO was used as a solvent to make 10mM FQ solution. No precipitate was observed. The separation result was shown in Fig 2.7. The same running conditions were used as those of Fig 2.5 and Fig 2.6. It can be found that the intensity of the two peaks for DMSO is lower than that for water as solvent. It might be partially because the solvents affected the mobility of FQ and the labeling reaction in DMSO was not as adequate as that in water. For the following experiment, water was used as the solvent for making the FQ solution.
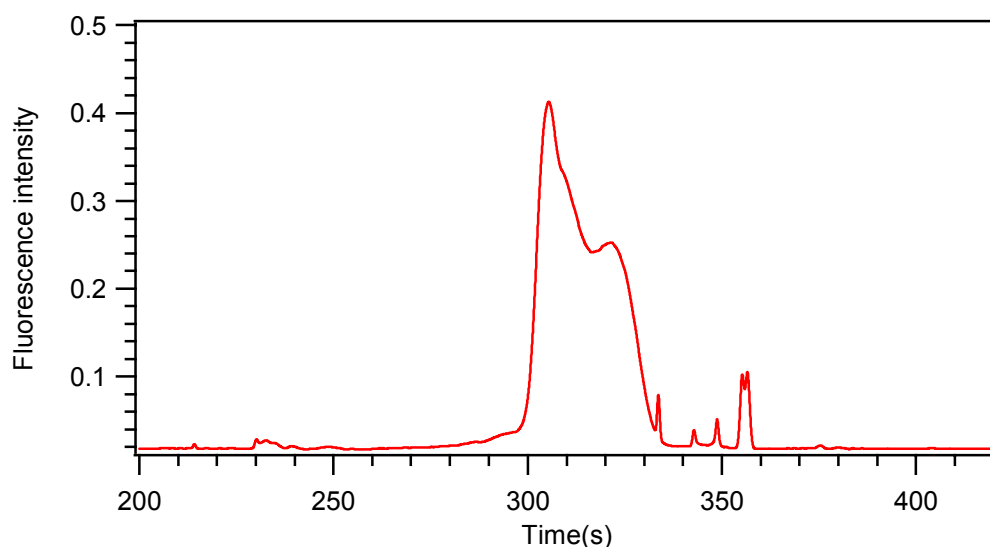
59
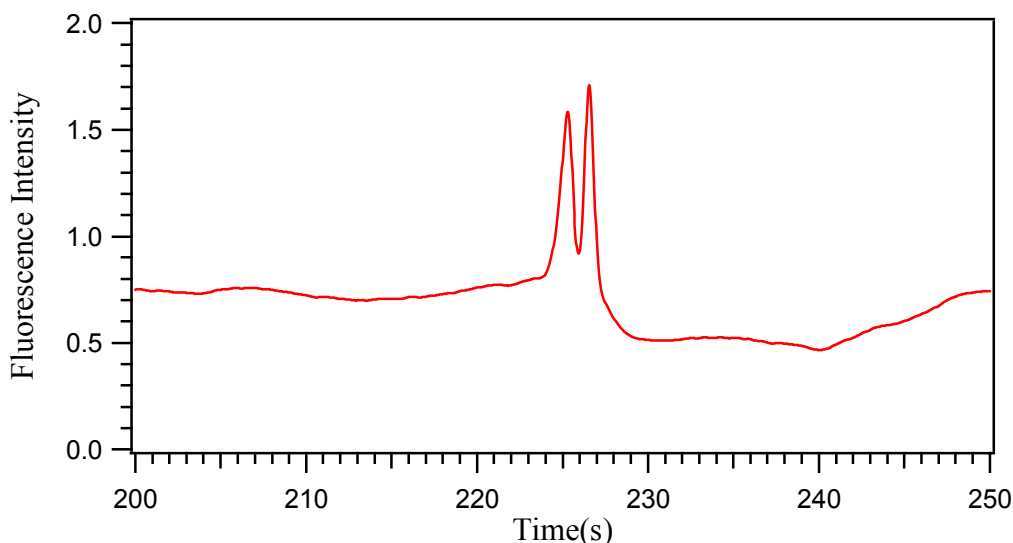
Figure2.7 Electropherogram for 1.6 µM lysozyme and 2.0µM myoglobin;

FQ on-column labeling in DMSO; Electric field strength of 400 V/cm;

The buffer of 2.5mM borax and 5mM SDS with a pH of 9.5;

Detection distance of 28 cm

2.9.3 Comparison of Different Capillary Lengths

The separation performance of a longer capillary length of 60cm with a detection distance of 40cm was compared with that of the former capillary with 42 cm capillary length and 28cm detection distance. The following consistent conditions were used: on-column labeling; the sample of 1.6 µM lysozyme and 2.0µM myoglobin in the buffer of **2**.5mM borax and 5mM SDS with a pH of 9.5 ; electric field strength: 400V/cm; hydrodynamic injection: vertical displacement of 10cm for 20s.

The separation result using the 60cm capillary with 48cm detection distance was given in Fig 2.8. Compared with Fig2.5, under the same electric field strength, band broadening dominated separation at this longer capillary length. Very poor resolution between the two components was observed. Therefore, for further experiments, the 42cm length of capillary with 28 cm detection distance was used and on-column labeling was taken.
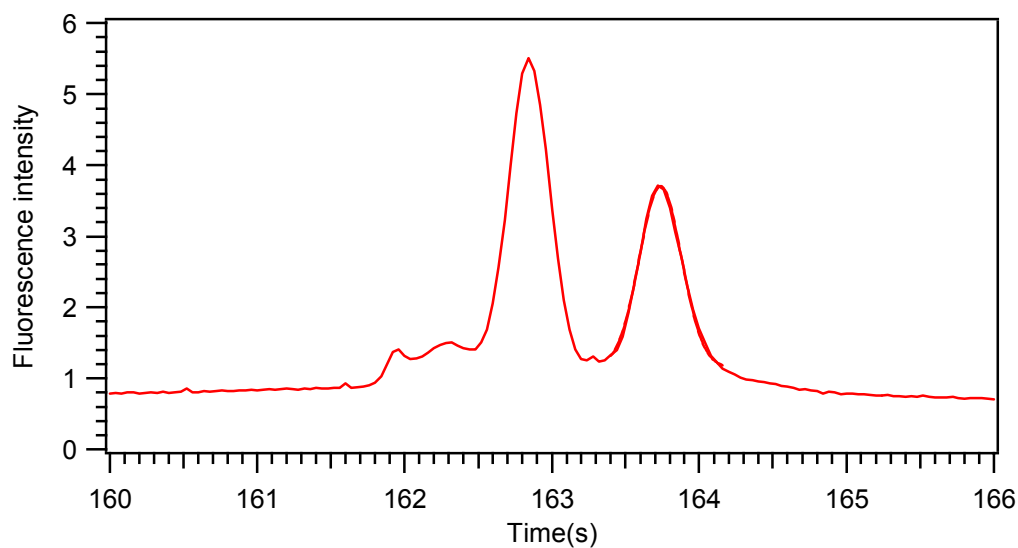
Figure 2.8 Electropherogram for 1.6 μM lysozyme and 2.0μM myoglobin;

FQ on-column labeling; Electric field strength of 400 V/cm;

The buffer of 2.5mM borax and 5mM SDS with a pH of 9.5;

Detection distance of 48 cm

2.9.4 Comparison of Different Electric Field Strengths

The separation performance at the higher electric field strength of 500V/cm was compared with that of 400V/cm whose separation result was given in Fig 2.5.The following consistent running conditions were used: on-column labeling; the sample of 1.6 μM lysozyme and 2.0μM myoglobin in the buffer of **2**.5mM borax and 5mM SDS with a pH of 9.5; capillary length: 42cm; detection distance: 28cm; electric field strength: 500V/cm; hydrodynamic injection: vertical displacement of 10cm for 20s.

Fig 2.9 gives the separation result at 500v/cm. It is seen clearly that at the higher electric field strength, much better separation efficiency and much better resolution were achieved. Approximately 1.4 million theoretical plate counts were demonstrated. A separation resolution for the two proteins within the range of two seconds was achieved.

Figure 2.9 Electropherogram for 1.6 µM lysozyme and 2.0µM myoglobin;

Electric field strength of 500V/cm; FQ on-column labeling;

The buffer of 2.5mM borax and 5mM SDS with a pH of 9.5;

Detection distance of 28 cm

2.10 Conclusions and Future Work

On-column fluorescence labeling is a very feasible method for CE separation. Under suitable experimental conditions, excellent separation performance with about 1.4 million theoretical plate numbers was achieved using on-column fluorescence labeling.

Future studies will employ a mixture of more types of standard proteins with different mobility to check on and further optimize the running conditions, such as electric field strength, separation distance. Then real samples will be able to be separated and analyzed using this setup and the optimized separation conditions.

CHAPTER 3 References

(1) Ouellette, J. *The Industrial Physicist,* August/September, 2003.

(2) Manz, A.; Graber, N.; Widmer, H.M. *Sens. Actuaors* 1990, B1, 244-248.

(3) Khandurina, J. etc. *Anal.Chem.* 2000, 72, 2995-3000.

(4) Manz, A. etc. *Sens. Actuators* 1990, B1, 249-255.

(5) Lab Chip, 2006, 6, 1118-1121.

(6) Snits, J.G. *Sens. Actuators, A* 1990, 21, 203-206.

(7) Esashi, M. *Sens. Actuators, A* 1990, 21, 161-167.

(8) Harrison, D.J.; Manza, A.; Fan, Z. H.; Ludi, h.; Widmer, H.M. *Anal.Chem.* 1992, 64, 1926-1932.

(9) AurouxP.A.; Iossifidis, D.; Reyes, D. R.; Manz, A. *Anal.Chem.* 2002, 74, 2637-2652.

(10) Jung, B.; Bharadwaj, R.; Santiago, J.G. *Anal.Chem.* 2006, 78, 2319-2327.

(11) Woolley, A.T.; Sensabaugh, G.F.; Mathies, R. A. *Anal.Chem.* 1997, 69, 2181-2186.

(12) Moore, A.W.; Jacobson, S.C.; Ramsey, J.M. *Anal. Chem.* 1995, 67, 4184-4189.

(13) Von Heeren, F.; Verpoorte, E,; Manz, A.;Thormann, W. *Anal.Chem.* 1996, 68, 2044-2053.

(14) Roman, G.T., Hlaus,T., Bass, K.J., Seelhammer, T.G., Culbertson, C.T. *Anal.Chem.* 2005, 77, 1414-1422.

(15) Kamholz, A.E., Weigl, B.H., Finlayson, B.A., Yager, P. *Anal.Chem.* 71, 5340-5347.

(16) Macounova, K., Cabrera, C.R., Holl, M.R., Yager, P. *Anal. Chem.* 72, 3745-3751.

(17) Hadd, A.G., Jacobson, S.C, Ramsey, J.M. *Anal.Chem.*71, 5206-5212 (1999).

(18) Sohn, L.L. et al. *Proceedings of the National Academy of Sciences of the United States of America* 97, 10687-10690(2000).

(19) Cheng, S.B. et al. *Anal. Chem.* 73, 1742-1479(2001).

(20) Yang, T. L., Jung, S. Y., Mao, H.B., Cremer, P.S. *Anal. Chem.* 73,165-169 (2001).

(21) Buchholz, B.A. et.al. *Anal. Chem.* 73, 157-164 (2001).

(22) Fan,Z.H. et.al. *Anal.Chem.* 71, 4851-4859 (1999).

(23) Glasgow, I.K. et.al. *Ieee Transactions on Biomedical Engineering* 48, 570-578(2001).

(24) Yang, J., Huang, Y., Wang, X.B., Becker, F.F., Gascoyne, P.R.C. *Anal.Chem.* 71, 911-918 (1999).

(25) Folch, A., Jo, B.H., Hurtado, O., Beebe, D.J., Toner, M. J. *Biom. Mate. Research* 52, 346-353 (2000).

(26) Liang, Z.; Chiem, N.; Ocvirk, G.; Tang, T.; Fluri, K.; Harrison, D.J. *Anal. Chem.* 1996, 68, 1040-1046.

(27) Chervet, J.P.; Van Soest, R.E.J.; Ursem, M. *J. Chromtogr.* 1991, 543, 439-449.

(28) Kutter, J.P.; Ramsey, R.S.; Jacobson, S.C.; Ramsey, J. M. *J. Microcolumn Sep.* 1998, 10,313-319.

(29) Lichtenberg, J.; Verpoorte, E,;de Rooij, N.F. *Electrophoresis* 2001, 22, 258-271.

(30) Gong, M.; Wehmeyer, R.; Limbach, W.P.; Arias, F.; Heineman, W. *Anal.Chem.* 2006, 78, 3730-3737.

(31) Pickering, L.W.; Baldock, S.J.; Fielden, P.R.; Goddard, N.J.; Snook, R.D.; Btown, B. J.T. *In Proceedings of Micro Total Analysis Systems,* 1998, 101-104.

(32) VanderNoot, V.A.; Hux, G.; Schoeniger, J.; Shepodd, T. *In Proceedings of Micro Total Analysis Systems,* 2001, 127-128.

(33) Figeys,D.; Aebersold, R. *Anal.Chem.* 1998, 70, 3721-3727.

(34) Kim,S.M.; Burns, M. Hasselbrink, E.F. *Anal. Chem.* 2006, 78, 4779-4785.

(35) Mala, Z.; Krivankova, L.; Gebauer, P.; Bocek, P. *Electrophoresis* 2007, 28, 243-253.

(36) M.H.V. Mulder, Basic principles of Membrane Technology, 2nd edn, *Kluwer Academic Publishers, Dordrecht, The Netherlands,* 2000.

(37) Khandurina, J.; Jacobson, S.C.; Waters, L.C.; Foote, R.S.; Ramsey, J.M. *Anal.Chem.* 1999, 71, 1815-1819.

(38) Khandurina, J.; McKnight, T. E.; Jacobson, S.C.; Waters, L.C.; Foote, R.S.; Ramsey, J.M. *Anal.Chem.* 2000, 72, 2995-3000.

(39) Foote, R.S.;Khandurina, J.; Jacobson, S.C.; Ramsey, J.M. *Anal.Chem.* 2005, 77, 57-63.

(40) Yu, C.; Davey,M.H.; Svec, F.; Frechet, J. M.J *Anal.Chem.* 2001, 73, 5088-5096.

(41) Ikuta, K.; maruo, S.; Fujisawa, T.; Yamada, A. *MEMS* 1999, Orlando, Fl, January 17-21, 1999; pp 376-381.

(42) Jong, J.de; Lammertink, R.G.H.; Wessling, M. *Lab.Chip,* 2006,6, 1125-1139.

(43) Stafie, N.; Stamatialis, D.F.; Wessling , M. *Sep. Purif.Technol.,* 2005, 45(3), 220.

(44) Wijmans, J.G.; Baker, R.W. *J. Membr. Sci.* 2005, 249, 245-249.

(45) Randall, G.C.; Doyle, P. *Proc. Natl. Acad. Sci. U.S.A.* 2005, 102(31), 10813-10818.

(46) Leclerc, E.; Sakai, Y.; Fujii, T. *Biotechnol. Prog.* 2004, 20, 750-755.

(47) Vollmer, A.P.; Probstein, R.F.; Gilbert, R., Thorsen, T. *Lab. Chip.* 2005, 5(10), 1059-1066.

(48) Leach, A.M.; Wheeler, A.R.; Zare, R.N. *Anal. Chem.* 2003, 75, 967-972.

(49) Ro, K.W.; Lim, K.; Kim, H.; Hahn, J.H. *Electrophoresis* 2002, 23, 1129-1137.

(50) Eijkel, J.; Bomer, J.; Van den Berg, A. *Appl. Phys.Lett.* 2005 87, 103-114.

(51) Su, Y.C.; Lin, L. J. *Microelectromech. Syst.* 2004 13(1), 75-82.

(52) Wang, P.C.; DeVoe, D.L.; Lee, C.S. *Electrophoresis* 2001, 22, 3857-3867.

(53) Jiang, Y.; Lee, C.S. *J. Chromatogr., A,* 2001, 924(1-2), 315.

(54) Wang, P.C.; Gao, J.; Lee, C.S. *J. Chromatogr.*, A, 2002, 942,115-122.

(55) Metz, S.; Trautmann, C.; Bertsch, A.; Renaud, P. J. *Micromech. Microeng.,* 2004, 14, 324-331.

(56) Kelly, R.T.; Li, Y.; Woolley, A.T. *Anal.Chem.* 2006, 78 (8), 2565-2570.

(57) Heyderman, L.J.; Ketterer, B.; Bachle, D.; Glaus, F.; Haas, B.; Schift, H.; Vogelsang, K.; Gobrecht, J.; Tiefenauer, L.; Dubochet, O. *Microelectron. Eng.* 2003, 67-68,208.

(58) Cui, T.; Fang, J.; Zheng, A.; Jones, F.; Reppond, A. *Sens. Actuators, B,* 2000, 71, 228-231.

(59) Yegung, K.L.; Zhang, X.; Lau, W.N.; Martin-Aranda, R. *Catal. Today,* 2005, 110 (1-2), 26.

(60) Tjerkstra, R.W.; Gardeniers, J.G.E.; Kelly, J.J.; Van den Berg, A. *J.Microelectromech. Syst.,* 2000, 9 (4), 495-501.

(61) Moorthy, J.: Beebe, D.J.; *Lab Chip,* 2003, 3(2), 62-66.

(62) Song, S.; Singh, A.K.; Kirby, B.J.; *Anal.Chem.,* 2004, 76,4589-4592.

(63) Song, S.; Singh, A.K.; Shepodd, T.J.; Kirby, B.J.; *Anal.Chem.,* 2004, 76, 2367-2373.

(64) Hisamoto, H.; Shimizu, Y.; Uchiyama, K.; Tokeshi, M.; Kikutani, Y.; Hibara, A.; Kitaori, T.; *Anal. Chem.,* 2003, 75, 350-354.

(65) Malmstadt, N.; Nash, M.A.; Purnell, R.F.; Schmidt, J.J. *Nano Lett.* 2006, 6 (9), 1961-1965.

(66) Moskvin, L.N.; Gurskii, V.S. Zh. *Anal. Khim.,* 1988, 43(4), p581.

(67) Moskvin, L.N.; Nikitina, T.G. *Membrane, Ser. Krit. Tekhnol.,* 2000, 8, p3

(68) Van de Nerbel, N.C.; Hajeman, J.J.; Brinkman, U.A.Th., *J. Chromatogr.,* 1993, 634, 1.

(69) Van de Nerbel, N.C.; *J. Chromatogr.,* 1999, 856, p55.

(70) Valcarcel, M., Arce, L., Rios, A., *J. Chromatogr.,* 2001, 924, p.3.

(71) Moskvin, L.N.; Nikitina, T.G. *J.Anal.Chem.* 2004, 59(1), 2-16.

(72) Lichtenberg, J.; De Rooij, N.F.; Verpoorte, E. *Talanta,* 2002, 56(2), 233-266.

(73) Peterson, D.S. *Lab Chip,* 2005, 5, 132-139.

(74) Handbook on biopolar membrane technology, ed. A.J.B. Kemperman, Twente University Press, Enschede, The Netherlands, 2000.

(75) Klein, L.C. *Noyes, Park Ridge, N.J.,* 1988, p.382.

(76) Avnir, D. *Acc. Chem. Res.* 1995, 28,328

(77) Lev, O.; Tsionsky, M.; Rabinovich, L. Glezer, V.; Sampath, S.; pankratov, I.; Gun, J. *Anal. Chem.* 1999, 67, 22A.

(78) Collinson, M.M. *Crit. Rev. Anal. Chem.* 1999, 29, 289.

(79) Brinker, C.J.; Scherer, G.W. *Sol-gel Sceince. Academic:* New York, 1989, P2.

(80) Martin-Brown, S.; Collinson, M.M. *Thesis of M.S.* KSU, 2004.

(81) Malik, A. *Electrophoresis* 2002, 23, 3973-3992.

(82) Hench, L.L.; West, J.K. *Chem. Rev.* 1990.90.33.

(83) Brinker, C.J.; Scherer, G.W. *Sol-gel Sceince. Academic:* New York, 1989, P.460.

(84) Ibid, p.465.

(85) Ibid, p.469.

(86) Brinker, C.J.; Scherer, G.W. *Sol-gel Sceince. Academic:* New York, 1989, P453.

(87) Nogami, M.; Suzuki, S.; Nagaska, K. J. *Non-cryst. Solids* 1991, 135,182.

(88) Avnir, D.; Braun, S.; Lev, O.; Ottolenghi, M. *Chem. Mater.* 1994, 6, 1605.

(89) Lai, D.C.; Dunn, B.; Zink, J.I. *Inorg. Chem.* 1996, 35, 2152.

(90) Darder, M.; Colilla, M.; Lara, N.; Ruiz-Hitaky, E. J. *Mater. Chem.* 2002, 12, 3660.

(91) Guizard, C. Fundamentals of inorganic membrane science and technology; Elsevier Science B.V. 1996.

(92) Collinson, M.M. *Mikrochim.Acta* 129, 1998, 149-165.

(93) Schubert, U.; Husing,N.; Lorenz, A. *Chem. Mater.* 1995, 7, 2010.

(94) Collinson, M.M. *Trends Anal. Chem.* 2002, 21, 30.

(95) Celzard, A.; Mareche, J.F. *J.Chem. Educ.* 2002, 79,854.

(96) Brinker, C.J.; Ward, T.L.; Sehgal, R.; Raman, N.K.; Hietala, S.L.; Smith, D.M.; Hua, D.W.; Headley, T.J. *J.Membr. Sci.*, 1993, 77, 165.

(97) De Lange, R.S.A. et al. *J. Sol-Gel Sci.Tech.*, 1994, 2, 489.

(98) Guizard, C.; Cygankiewicz, N.; Larbot, A.; Cot, L. J.*Non-Cryst. Solids,* 1986, 82, 86.

(99) Guizard, C.; Larbot, A.; Cot, L.; Perez, S.; Rouviere, J.; Etude de la. *J.Chim. Phys.,* 1990, 87, 1901.

(100) Brinker, C.J.; Sehgal, R.; Raman, N.; Schunk, P.R.; Headley, T.J. J.Sol-Gel Sci. Techol.; 1994,2,469.

(101) Khaledi, M.G.; High Performance Capillary Electrophoresis; John Wiley&Sons, NY, 1998.

(102) Pu, Q; Yun, J; Temkin, H; Liu, S. Nano Lett., 2004, 4, 1099-1103.

(103) Camilleri, P. Capillary Electrophoresis: Theory and Practice; CRC Press; Boca Raton, 1993.

(104) Kuhn, R.; Hoffstetter-Kuhn, S. Capillary Electrophoresis: Principles and Practice; Springer-Verlag: Berlin, 1993.

(105) Landers, J.P. Handbook of Capillary Electrophoresis; CRC Press: Boca Raton, 1994.

(106) leube, J.; Roechel, O. *Anal.Chem.* 1994, 66, 1090.

(107) Kasicka, V. *Electrophoresis* 2006, 27, 142-175.

(108) Janini, G.M.; Conrads, T.P.; Veenstra, T.D.; Issaq, H.J.; *J. Chromatogr. B* 2003, 787, 43-51.

(109) Fujiwara, S.; Honda, S. *Anal. Chem.* 1986, 58, 1811-1814.

(110) Huang, X.; Luckey, J. A.; Gordon, M.J.; Zare, R. N. *Anal. Chem.* 1989, 61, 766-770.

(111) Dose, E.V.; Guiochon, G.A. *Anal. Chem.* 1991, 63, 1154-1158.

(112) Kvasnicka, F. J.*Sep.Sci.* 2005, 28, 813-825.

(113) Sung, W.; Chen, S. *Electrophoresis* 2006, 27, 257-265.

(114) Kraly, J.; Fazal, M.A.; Schoenherr, R.M.; Bonn, R.; Harwood, M.M.; Turner, E.; Jones, M.; Dovichi, N.J. *Anal. Chem.* 2006, 78, 4097.

(115) Ahmadzadeh, H.; Krylov, S. *Methods in Mol. Bio.* 276, 29-38.

(116) Pinto, D.M.; Arriaga, E. A.; Craig, D.; Angelova, J.; Sharma, N.; Ahmadzadeh, h.; Dovivhi,N.J. *Anal.Chem.* 1997, 69, 3015-3021.

(117) Hu, Sh., Dovichi, N.J. *Current opinion in Chem. Bio.* 2003, 7, 603-608.

(118) Beale, S., Hsieh, Y., Wiesler, D. Novotny, M. *J. Chrom.* 1990, 499, 579-587.